Inorganic Chemistry

Article

pubs.acs.org/IC

Ir(2-Phenylpyridine)$_2$(benzene-1,2-dithiolate) Anion as a Diastereoselective Metalloligand and Nucleophile: Stereoelectronic Effect, Spectroscopy, and Computational Study of the Methylated and Aurated Complexes and their Oxygenation Products

Van Ha Nguyen, Rebecca Shu Hui Khoo, and John H. K. Yip*

Department of Chemistry, National University of Singapore, 3 Science Drive 3, Singapore, 117543

Supporting Information

ABSTRACT: The anionic complex [Ir(2-phenylpyridine)$_2$-(benzene-1,2-dithiolate)]$^-$ ([**IrSS**]$^-$) is a nucleophile and metalloligand that reacts with methyl iodide and AuPR$_3^+$ (R = Ph or Et) to form S-methylated complexes (thiother−thiolate and dithiother complexes) and S-aurated complexes, respectively. The reactions are completely diastereselective, producing only the enantiomers ΛS and ΔR or ΛSS and ΔRR. The diastereoselectivity is stereoelectronically controlled by the orientation of the highest occupied molecular orbital (HOMO) of [**IrSS**]$^-$ arising from filled dπ−pπ antibonding interactions, and the chirality of the iridium ion. Methylation or auration removes the high-energy lone pair of the thiolate S atom, leading to low-lying HOMOs composed mainly of the Ir d-orbital and the 2-phenylpyridine π (ppyπ) orbital. The methylated and aurated complexes can be oxidized by H_2O_2 or peracid to give sulfinate−thiother, disulfoxide, and sulfinate−sulfoxide complexes, and the oxygenation further stabilizes the HOMO. All the complexes are luminescent, and their electronic spectra are interpreted with the aid of time-dependent density functional theory calculations. The thiother−thiolate complex exhibits ligand(S)-to-ligand(π* of ppy)-charge-transfer/metal-to-ligand-charge-transfer absorption (LLCT/MLCT) and a relatively low-energy ^{3}LLCT/MLCT emission, while the other complexes display ^{3}ππ*/MLCT emissions.

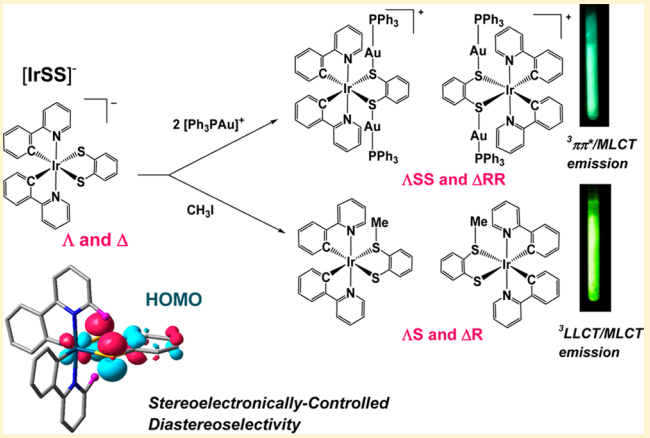

INTRODUCTION

A metal complex containing ligands L with free lone pairs can in principle act as a ligand (metalloligand) or a nucleophile (Scheme 1). The donor ability or nucleophilicity of such a complex depends on the electronic properties of M and L. Usually, strong electron-donating ability results from combining d^6 or d^8 metal ions, which have completely filled dπ orbitals with relatively electropositive chalcogenides[1] or pnictogenides.[2] In 1970, Chatt demonstrated that [Pt$_2$(μ-S)$_2$(L)$_4$] (L = PMePh$_2$) is a nucleophile that reacts with an alkyl halide (RX) to form [Pt$_2$(μ-S)(μ-SR)(L)$_4$]$^+$.[3] Mingos and later Hor further established that a similar complex [Pt$_2$(μ-S)$_2$(PPh$_3$)$_4$] is a metalloligand that can coordinate to various metal ions via its sulfide groups.[1e,g,4]

Scheme 1

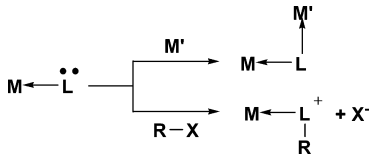

Sulfide and thiolate are common lone-pair donors in metalloligands. For example, intermolecular M−S bond formation between planar [M(S^S)$_2$]$^-$ molecules (M = Co^{3+}, Mn^{3+}, or Fe^{3+} and S^S = dithiolate or dithiolene) leads to the polymeric structures in their crystals.[5] Of particular relevance to the present study is Konno's work, which describes the self-assembly of the metalloligand [Co(aet)$_3$] (aet = 2-aminoethanethiolate) and Pd^{2+}, Au$^+$, or Ag$^+$ ions into chiral supramolecules.[6]

It is known that some late transition metal thiolate complexes are highly nucleophilic. Enemark and Lichtenberger[7] observed enhanced nucleophilicity of the coordinated phenylthiolate in the complex CpFe(CO)$_2$SR, which was attributed to destabilization of a lone pair on the S atom by filled−filled antibonding between the dπ orbitals of d^6 Fe^{2+} and the lone pair, the so-called filled dπ−pπ interactions.[8] Similarly, thiolates of other "t$_{2g}$-rich" ions such as Ni^{2+}, Ru^{2+}, and Zn^{2+} were shown to be nucleophilic.[1k,8b,9−11]

In a recent study, we combined the well-known luminophore Ir^{3+}(ppy)$_2$ (ppy = 2-phenylpyridine) with benzene-1,2-dithiolate

Received: December 2, 2014
Published: February 18, 2015

DOI: 10.1021/ic502875y
Inorg. Chem. 2015, 54, 2264−2277

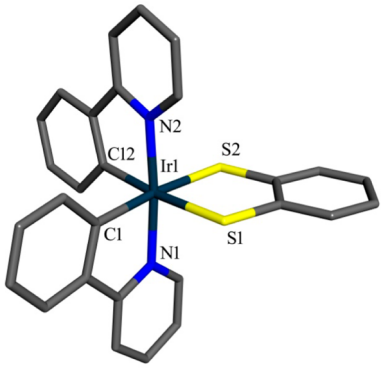

Figure 1. DFT optimized structure of $[\mathbf{IrSS}]^-$.

to form anionic $[Ir(ppy)_2(benzene\text{-}1,2\text{-}dithiolate)]^-$ ($[\mathbf{IrSS}]^-$, Figure 1). The $[\mathbf{IrSS}]^-$ complex was found to be very prone to dioxygenation, yielding the monosulfinate $[\mathbf{IrSSO_2}]^-$ and disulfinate $[\mathbf{IrSO_2SO_2}]^-$ complexes (Scheme 2).[12]

Our findings indicate that the thiolate S atoms of $[\mathbf{IrSS}]^-$ are highly electron-rich, suggesting that the complex could act as a metalloligand and a nucleophile. This property is demonstrated in the present study through reacting the complex with $Au^I(phosphine)^+$ ion and methyl iodide (Scheme 3).

As $[\mathbf{IrSS}]^-$ has helical chirality (Δ or Λ) and the S atoms are prochiral, addition of metal ions or alkyl groups to the S atoms would lead to the formation of enantiomers and diastereomers (Scheme 4). Single and double additions would give rise to two pairs ΛR, ΔS and ΛS, ΔR and three pairs ΛRR, ΔSS, ΛSS, ΔRR, and ΛRS and ΔSR of enantiomers, respectively.

Stereoelectronic effects, common for organic reactions, are scarcely observed in inorganic and organometallic transformations. Our results show that the methylation and auration are completely diastereoselective, producing only one pair of the enantiomers, and the diastereoselectivity is stereoelectronically controlled.

The complex $[\mathbf{IrSS}]^-$ was originally designed to be a luminescent probe for reactive oxygen species. Indeed, dioxygenation of the thiolate S atoms leads to a blue shift of the emission color. However, the complex, being too strongly reducing, reacts with O_2 almost instantaneously. We envisioned that alkylation of the thiolate could tame the reactivity of the

Scheme 2

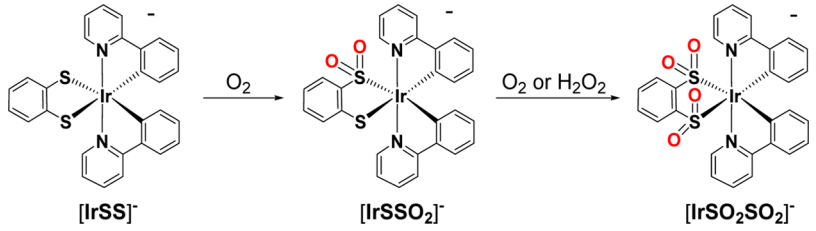

Scheme 3

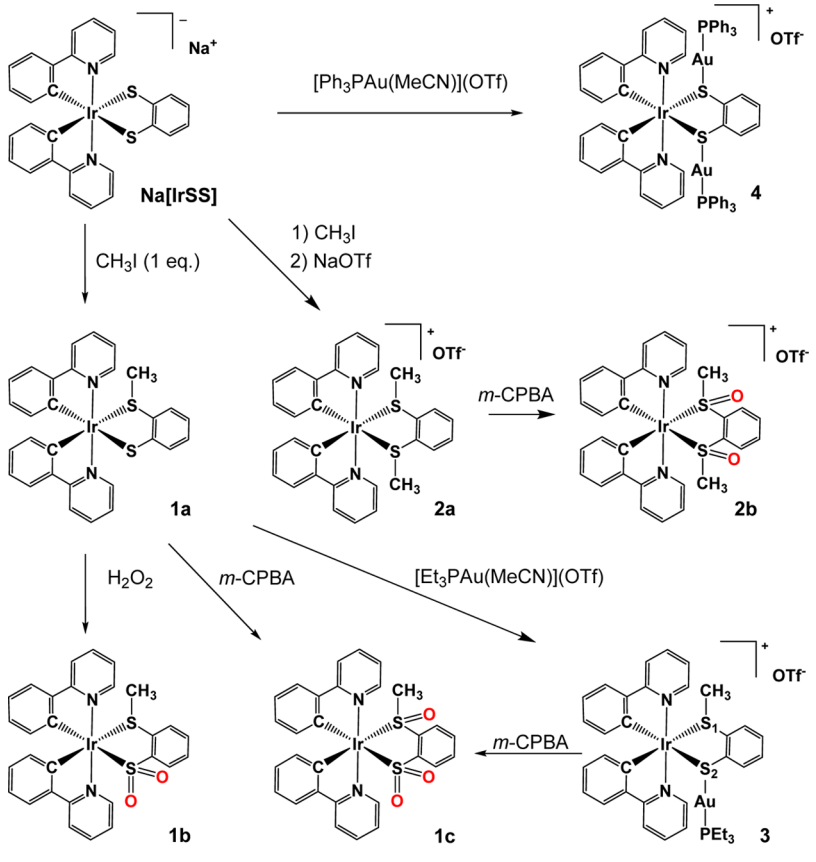

DOI: 10.1021/ic502875y
Inorg. Chem. 2015, 54, 2264−2277

Scheme 4

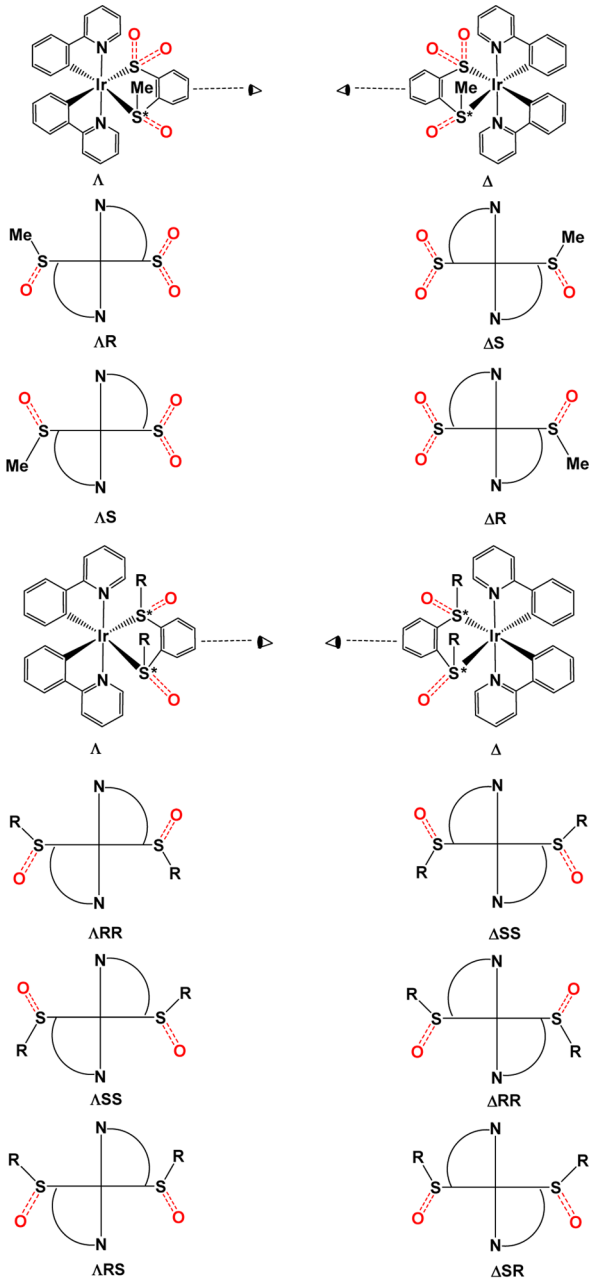

R = Me or AuL (L = PPh_3 or PEt_3)

complex toward O_2. Our study shows that the methylated and aurated complexes do not react with O_2 but are still reactive toward H_2O_2 or peracid, forming sulfoxides or sulfinates upon oxidation (Scheme 3). We probed the changes in electronic structures and photophysical properties of the complexes brought about by alkylation, metalation, and oxidation by using absorption and emission spectroscopy and rationalized those changes with density functional theory (DFT) calculations.

EXPERIMENTAL SECTION

General Methods. All syntheses were carried out in an Ar atmosphere. Solvents used for syntheses and spectroscopic measurements were purified according to the literature procedures.[13] $Ir_2(ppy)_4(\mu\text{-}Cl)_2$,[14] Et_3PAuCl,[15] and Ph_3PAuCl[16] were prepared according to reported methods. Silver trifluoromethanesulfonate (AgOTf), sodium trifluoromethanesulfonate (NaOTf), *m*-chloroperoxybenzoic acid (*m*-CPBA), aqueous solution of H_2O_2 (30%), and benzene-1,2-dithiol were obtained from Aldrich and used without prior purification. ***Caution!*** *m-Chloroperoxybenzoic acid may cause fire when heated.*

Physical Methods. The UV−vis absorption and emission spectra of the compounds were recorded on a PerkinElmer Lambda 750 spectrophotometer and a Horiba FluoroMax-4 fluorescence spectrophotometer, respectively. Emission lifetimes were measured on a Horiba Jobin-Yvon Fluorolog FL-1057 instrument, and 9,10-diphenylanthracene was used as a standard for quantum yield measurements. Solutions for emission spectrum, lifetime, and quantum yield measurements were degassed by five freeze−pump−thaw cycles. ^1H and $^{31}P\{^1H\}$ NMR spectra were obtained on a BrukerAvance 500 spectrometer. All chemical shifts are quoted relative to $SiMe_4$ (^1H) or H_3PO_4 (^{31}P). Electrospray ionization mass spectra (ESI-MS) were obtained using a Finnigan LCQ spectrometer. Isotopic distributions were simulated by the Isotope Viewer utility in Xcalibur (Thermo Scientific) software package. Infrared spectra (Nujol mulls) were obtained using a Bruker Alpha spectrometer. Elemental analyses were carried out at the Elemental Analysis Laboratory in the Department of Chemistry, National University of Singapore.

Na[Ir(ppy)$_2$(Benzene-1,2-dithiolate)] (Na[IrSS]). $Ir_2(ppy)_4(\mu\text{-}Cl)_2$, (107 mg, 0.1 mmol) was stirred with AgOTf (57 mg, 0.2 mmol) in acetonitrile (MeCN, 30 mL) for 2 h. The mixture was filtered, and the pale yellow solution was transferred into another Schlenk flask containing benzene-1,2-dithiol (31 mg, 0.2 mmol) and NaOH (35.2 mg, 0.88 mmol) in methanol (MeOH, 30 mL). The solution turned from yellow to red and was stirred overnight under argon to give a deep red solution of Na[**IrSS**], which was sensitive to air and was used without isolation. Addition of $^nBu_4NCl$ precipitated the complex as [Bu_4N][**IrSS**], which was fully characterized in our previous study.[12]

*Ir(ppy)$_2$(Benzene-1-thioether-2-thiolate) (**1a**).* Methyl iodide (MeI) (28 mg, 0.2 mmol) in MeOH (30 mL) was added dropwise to a freshly prepared solution of Na[**IrSS**] (0.2 mmol). The color of the solution slowly changed from deep red to orange, and finally a yellow suspension resulted after stirring for 5 h. The solvent was removed, and the yellow precipitate was washed successively with H_2O and MeOH. Single crystals were obtained by slow evaporation of an MeCN solution of the complex. Yield: 89 mg, 68%. Anal. Calcd (%) for **1a** ($C_{29}H_{23}IrN_2S_2$): C, 53.11; H, 3.53; N, 4.27. Found: C, 52.72; H, 3.53; N, 4.22. ^1H NMR (500 MHz, CD_3CN) δ 9.75 (d, $^3J_{H2-H1(H2'-H1')}$ = 5.9 Hz, 1H, $H_{1(1')}$), 8.75 (d, $^3J_{H2'-H1'(H2-H1)}$ = 5.9 Hz, 1H, $H_{1'(1)}$), 8.01−8.05 (2H, H_4, $H_{4'}$), 7.89 (t, $^3J_{H4-H3(H4'-H3')}$ = $^3J_{H2-H3(H2'-H3')}$ = 7.8 Hz, 1H, $H_{3(3')}$), 7.83 (t, $^3J_{H4'-H3'(H4-H3)}$ = $^3J_{H2'-H3'(H2-H3)}$ = 7.8 Hz, 1H, $H_{3'(3)}$), 7.76 (d, $^3J_{H6-H5(H6'-H5')}$ = 7.2 Hz, 1H, $H_{5(5')}$), 7.69 (d, $^3J_{H6'-H5'(H6-H5)}$ = 7.7 Hz, 1H, $H_{5'(5)}$), 7.48 (d, $^3J_{H11-H12}$ = 7.9 Hz, 1H, H_{12}), 7.38 (d, $^3J_{H10-H9}$ = 7.9 Hz, 1H, H_9), 7.28 (dd, $^3J_{H3-H2(H3'-H2')}$ = 7.8 Hz, $^3J_{H1-H2(H1'-H2')}$ = 5.9 Hz, 1H, $H_{2(2')}$), 7.17 (dd, $^3J_{H3'-H2'(H3-H2)}$ = 7.8 Hz, $^3J_{H1'-H2'(H1-H2)}$ = 5.9 Hz, 1H, $H_{2'(2)}$), 6.92−6.98 (2H, $H_{6(6')}$, H_{11}), 6.81−6.89 (3H, $H_{6'(6)}$, $H_{7(7')}$, H_{10}), 6.75 (t, $^3J_{H8'-H7'(H8-H7)}$ = $^3J_{H6'-H7'(H6-H7)}$ = 7.5 Hz, 1H, $H_{7'(7)}$), 6.48 (d, $^3J_{H7-H8(H7'-H8')}$ = 7.6 Hz, 1H, $H_{8(8')}$), 6.18 (d, $^3J_{H7'-H8'(H7-H8)}$ = 7.5 Hz, 1H, $H_{8'(8)}$), 1.57 (s, 3H, H_{Me}). ESI-MS: *m*/*z* 656.9 $[M + H]^+$.

*Ir(ppy)$_2$(Benzene-1-sulfinate-2-thioether) (**1b**).* **1a** (66 mg, 0.1 mmol) was stirred with excess aqueous H_2O_2 solution (30%, 2.0 mL, 20 mmol) in MeCN (30 mL) for 5 h to form a pale yellow solution. Rotoevaporation of the solution gave yellow solids, which were washed with water several times. Slow evaporation of a CH_2Cl_2/MeOH solution afforded single crystals. Yield: 56 mg, 81%. Anal. Calcd (%) for **1b** ($C_{29}H_{23}IrN_2S_2O_2$): C, 50.64; H, 3.37; N, 4.07. Found: C, 50.71; H, 3.57; N, 3.92. ^1H NMR (500 MHz, CD_3CN) δ 10.09 (d, $^3J_{H2-H1(H2'-H1')}$ = 5.8 Hz, 1H, $H_{1(1')}$), 8.50 (d, $^3J_{H2'-H1'(H2-H1)}$ = 5.7 Hz, 1H, $H_{1'(1)}$), 8.05−8.09 (2H, H_4, $H_{4'}$), 7.96 (t, $^3J_{H2-H3(H2'-H3')}$ = $^3J_{H4-H3(H4'-H3')}$ = 7.8 Hz, 1H, $H_{3(3')}$), 7.92 ($^3J_{H2'-H3'(H2-H3)}$ = $^3J_{H4'-H3'(H4-H3)}$ = 7.8 Hz, 1H, $H_{3'(3)}$), 7.77−7.82 (3H, $H_{5(5')}$, H_9, H_{12}), 7.74 (d, $^3J_{H6'-H5'(H6-H5)}$ = 7.9 Hz, 1H, $H_{5'(5)}$), 7.50−7.53 (2H, H_{10}, H_{11}), 7.33 (dd, $^3J_{H3-H2(H3'-H2')}$ = 7.8 Hz,

DOI: 10.1021/ic502875y
Inorg. Chem. 2015, 54, 2264−2277

Table 1. Crystal Data for 1a, 1b, 2a·MeCN, 2b·MeOH, 3, and 4·CH_2Cl_2

	1a	1b	2a·MeCN	2b·MeOH	3	4·CH_2Cl_2
empirical formula	$C_{29}H_{23}IrN_2S_2$	$C_{29}H_{23}IrN_2O_2S_2$	$C_{33}H_{29}F_3IrN_3O_3S_3$	$C_{32}H_{30}F_3IrN_2O_6S_3$	$C_{36}H_{38}AuF_3IrN_2O_3PS_3$	$C_{66}H_{52}Au_2Cl_2F_3IrN_2O_3P_2S_3$
formula weight	655.81	687.81	860.97	883.96	1120.00	1793.25
crystal system	orthorhombic	monoclinic	monoclinic	monoclinic	monoclinic	triclinic
space group	$P2_12_12_1$	$P2_1/n$	$P2_1$	$P2_1/c$	$P2_1/c$	$P\bar{1}$
a (Å)	9.2232(5)	8.695(9)	8.4194(4)	14.706(3)	16.4463(17)	13.214(11)
b (Å)	11.7387(6)	21.37(2)	14.8450(6)	14.367(3)	14.6413(16)	13.935(11)
c (Å)	22.4883(13)	13.006(13)	13.0152(6)	15.697(3)	17.6882(18)	19.374(16)
α (deg)	90	90	90	90	90	94.876(17)
β (deg)	90	93.16(2)	92.4500(10)	104.685(4)	116.593(2)	102.427(16)
γ (deg)	90	90	90	90	90	115.538(15)
volume (Å^3)	2434.8(2)	2413(4)	1625.23(13)	3208.2(10)	3808.6(7)	3079(4)
Z	4	4	2	4	4	2
density (calcd, g cm^{-3})	1.789	1.893	1.759	1.830	1.953	1.934
abs coefficient (mm^{-1})	5.676	5.737	4.357	4.423	7.597	7.208
$F(000)$	1280	1344	848	1744	2152	1720
crystal size (mm^3)	0.250 × 0.060 × 0.050	0.300 × 0.220 × 0.080	0.320 × 0.320 × 0.180	0.36 × 0.24 × 0.12	0.460 × 0.360 × 0.160	0.560 × 0.240 × 0.100
θ range for data collection (deg)	2.387−27.500	1.835−27.498	2.744−27.489	1.431−27.497	1.895−27.498	1.654−27.498
index ranges	$-11 \le h \le 11$, $-15 \le k \le 14$, $-29 \le l \le 29$	$-11 \le h \le 11$, $-27 \le k \le 23$, $-16 \le l \le 15$	$-10 \le h \le 10$, $-19 \le k \le 19$, $-16 \le l \le 16$	$-19 \le h \le 18$, $-18 \le k \le 18$, $-20 \le l \le 15$	$-21 \le h \le 21$, $-19 \le k \le 17$, $-22 \le l \le 17$	$-17 \le h \le 17$, $-18 \le k \le 18$, $-25 \le l \le 25$
no. reflections collected	35 508	16 734	27 083	22 391	26 896	40 206
no. independent reflections (R(int))	5577 (0.0379)	5529 (0.0621)	7156 (0.0268)	7368 (0.0415)	8712 (0.0467)	14092 (0.0496)
max., min transmission	0.7457, 0.5591	0.7456, 0.4827	0.5633, 0.4600	0.7456, 0.5578	0.7456, 0.5274	0.7456, 0.3340
no. data/restraints/parameters	5577/0/308	5529/0/326	7156/1/418	7368/376/354	8712/0/455	14092/0/757
final R indices[a] [$I > 2\sigma(I)$]						
$R1$	0.0201	0.0425	0.0136	0.0341	0.0310	0.0322
$wR2$	0.0369	0.0978	0.0484	0.0837	0.0790	0.0780
goodness-of-fit (GOF)[b]	1.027	1.074	1.115	1.103	1.074	1.031
largest diff. peak and hole (e Å^{-3})	1.273 and −0.331	2.757 and −1.529	0.759 and −1.139	1.814 and −0.959	2.285 and −0.855	2.415 and −1.042

[a] $R1 = (||F_o| - |F_c||)/(|F_o|)$; $wR2 = [w(F_o^2 - F_c^2)/w(F_o^4)]^{1/2}$. [b] $GOF = [(w(F_o^2 - F_c^2)^2/(n-p)]^{1/2}$. For crystal determination, the scan type and wavelength of radiation used are ω and 0.710 73 Å, respectively.

$^3J_{H1-H2(H1'-H2')}$ = 5.8 Hz, 1H, $H_{2(2')}$), 7.16 (dd, $^3J_{H3'-H2'(H3-H2)}$ = 7.8 Hz, $^3J_{H1'-H2'(H1-H2)}$ = 5.7 Hz, 1H, $H_{2'(2)}$), 6.96−7.02 (2H, H_6, $H_{6'}$), 6.81−6.88 (2H, H_7, $H_{7'}$), 6.34 (d, $^3J_{H7-H8(H7'-H8')}$ = 7.5 Hz, 1H, $H_{8(8')}$), 6.25 (d, $^3J_{H7'-H8'(H7-H8)}$ = 7.7 Hz, 1H, $H_{8'(8)}$), 1.78 (s, 3H, H_{Me}). ESI-MS: m/z 689.0 $[M + H]^+$.

*Ir(ppy)$_2$(Benzene-1-sulfinate-2-sulfoxide) (**1c**).* Excess *m*-chloroperoxybenzoic acid 77% (*m*-CPBA, 400 mg, 1.80 mmol) was added to a solution of **1a** (63 mg, 0.09 mmol) in CH_2Cl_2 (30 mL), and the mixture was stirred for 2 h to form a pale yellow solution. Rotoevaporation of the solvent gave solids, which were washed several times with Et_2O. The compound was recrystallized by diffusion of Et_2O into an MeCN solution. Yield: 34 mg, 53%. Anal. Calcd (%) for **1c** ($C_{29}H_{23}IrN_2S_2O_3$): C, 49.49; H, 3.29; N, 3.98. Found: C, 49.23; H, 3.13; N, 3.80. ^{1}H NMR (500 MHz, CD_3CN) δ 10.01 (d, $^3J_{H2-H1(H2'-H1')}$ = 6.1 Hz, 1H, $H_{1(1')}$), 9.02 (d, $^3J_{H2'-H1'(H2-H1)}$ = 6.0 Hz, 1H, $H_{1'(1)}$), 8.15−8.19 (2H, $H_{4(4')}$, H_{12}), 8.04−8.09 (2H, $H_{4'(4)}$, $H_{3(3')}$), 7.94 (t, $^3J_{H2'-H3'(H2-H3)}$ = $^3J_{H4'-H3'(H4-H3)}$ = 7.8 Hz, 1H, $H_{3'(3)}$), 7.87 (d, $^3J_{H10-H9}$ = 7.5 Hz, 1H, H_9), 7.83 (d, $^3J_{H6-H5(H6'-H5')}$ = 7.5 Hz, 1H, $H_{5(5')}$), 7.72−7.79 (3H, $H_{5'(5)}$, H_{10}, H_{11}), 7.40 (dd, $^3J_{H1-H2(H1'-H2')}$ = 6.1 Hz, $^3J_{H3-H2(H3'-H2')}$ = 7.5 Hz, 1H, $H_{2(2')}$), 7.16 (dd, $^3J_{H3'-H2'(H3-H2)}$ = 7.8 Hz, $^3J_{H1'-H2'(H1-H2)}$ = 6.0 Hz, 1H, $H_{2'(2)}$), 7.08 (t, $^3J_{H5-H6(H5'-H6')}$ = $^3J_{H7-H6(H7'-H6')}$ = 7.5 Hz, 1H, $H_{6(6')}$), 7.04 (t, $^3J_{H5'-H6'(H5-H6)}$ = $^3J_{H7'-H6'(H7-H6)}$ = 7.6 Hz, 1H, $H_{6'(6)}$), 6.93 (t, $^3J_{H6-H7(H6'-H7')}$ = $^3J_{H8-H7(H8'-H7')}$ = 7.5 Hz, 1H, $H_{7(7')}$), 6.88 (t, $^3J_{H6'-H7'(H6-H7)}$ = $^3J_{H8'-H7'(H8-H7)}$ = 7.6 Hz, 1H, $H_{7'(7)}$), 6.35 (d, $^3J_{H7-H8(H7'-H8')}$ = 7.5 Hz, 1H, $H_{8(8')}$), 6.09 (d, $^3J_{H7'-H8'(H7-H8)}$ = 7.6 Hz, 1H, $H_{8'(8)}$), 2.43 (s, 3H, H_{Me}). ESI-MS: m/z 705.0 $[M + H]^+$.

*[Ir(ppy)$_2$(Benzene-1,2-dithioether)](OTf) (**2a**).* Methyl iodide (66 mg, 0.44 mmol) was added to a freshly prepared solution of Na[**IrSS**] (0.2 mmol). The solution slowly turned from deep red to pale yellow. After the solution was stirred for 5 h, solvent was removed to obtain a yellow solid. The solid was dissolved in MeOH and filtered. Excess NaOTf was then added to the solution to precipitate the product. Crystals were obtained by slow diffusion of Et_2O into an MeCN solution of the product. Yield: 126 mg, 77%. Anal. Calcd (%) for **2a** ($C_{31}H_{26}IrN_2S_3F_3O_3$): C, 45.41; H, 3.20; N, 3.42. Found: C, 45.17; H, 3.27; N, 3.56. ^{1}H NMR (500 MHz, CD_3CN) δ 8.77 (d, $^3J_{H2-H1}$ = 5.7 Hz, 1H, H_1), 8.16 (d, $^3J_{H3-H4}$ = 7.8 Hz, 1H, H_4), 8.04 (t, $^3J_{H2-H3}$ = $^3J_{H4-H3}$ = 7.8 Hz, 1H, H_3), 7.93 (m, 1H, H_9), 7.81 (d, $^3J_{H6-H5}$ = 7.6 Hz, 1H, H_5), 7.59 (m, 1H, H_{10}), 7.34 (dd, $^3J_{H3-H2}$ = 7.8 Hz, $^3J_{H1-H2}$ = 5.8 Hz, 1H, H_2), 7.06 (t, $^3J_{H5-H6}$ = $^3J_{H7-H6}$ = 7.6 Hz, 1H, H_6), 6.92 (t, $^3J_{H6-H7}$ = $^3J_{H8-H7}$ = 7.6 Hz, 1H, H_7), 6.30 (d, $^3J_{H7-H8}$ = 7.6 Hz, 1H, H_8), 1.79 (s, 3H, H_{Me}). ESI-MS: m/z 671.0 $[M\text{-}OTf]^+$.

*[Ir(ppy)$_2$(Benzene-1,2-disulfoxide)](OTf) (**2b**).* Excess *m*-chloroperoxybenzoic acid 77% (*m*-CPBA, 890 mg, 4.0 mmol) was added to a solution of **2a** (66 mg, 0.08 mmol) in MeOH, and the mixture was stirred for 2 h to obtain a pale yellow solution. The solvent was removed by rotoevaporation to give solid, which was purified by recrystallization from an MeCN/Et_2O mixture. Crystals were obtained

DOI: 10.1021/ic502875y
Inorg. Chem. 2015, 54, 2264−2277

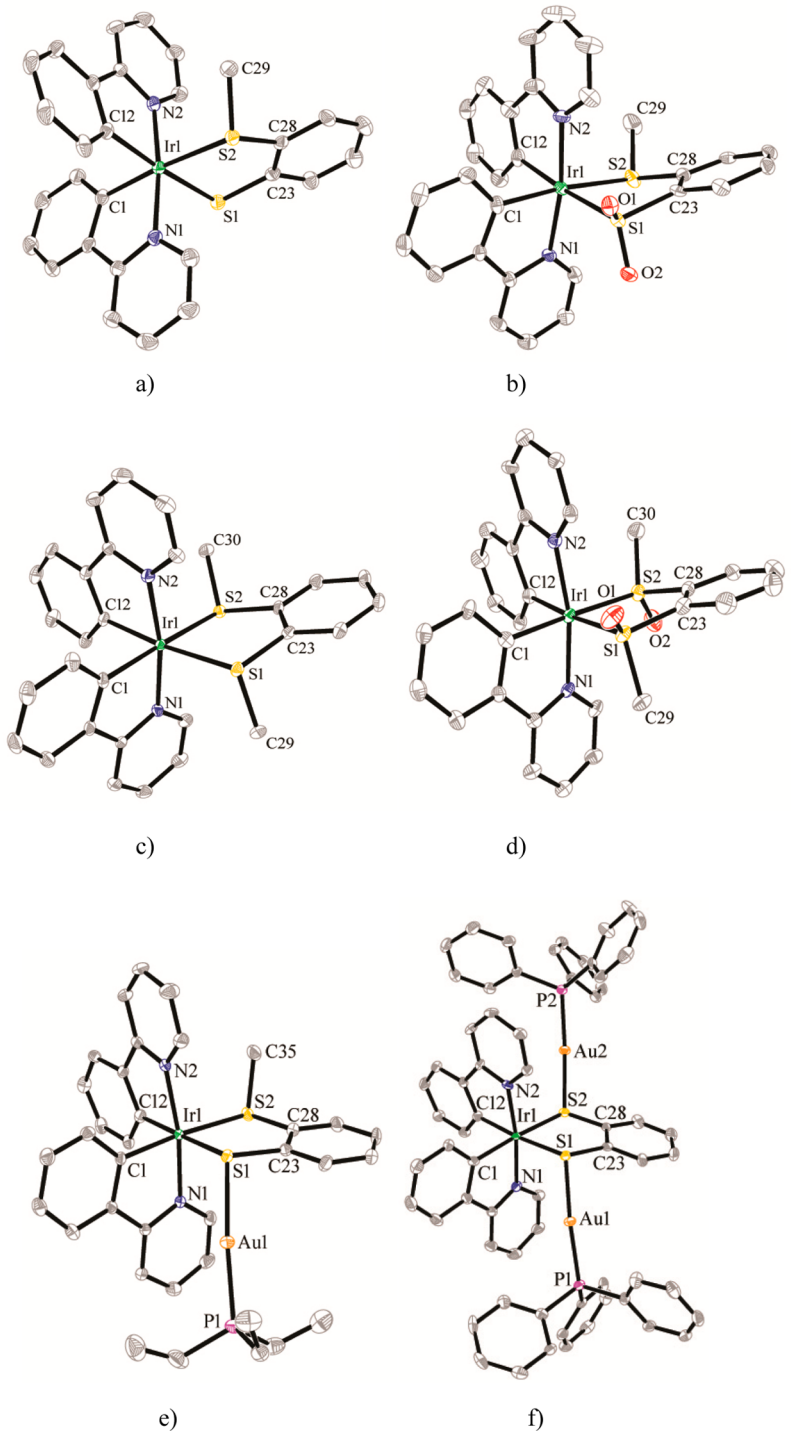

Figure 2. Perspective views of (a) ΔR **1a**, (b) ΛS **1b**, (c) ΛSS **2a**, (d) ΛSS **2b**, (e) ΛSS **3**, and (f) ΛSS **4**. Thermal ellipsoids drawn at 50% probability level; for **1b**, **2b**, **3**, and **4**, only the Λ isomers are shown. H atoms, anions, and solvent molecules are omitted. Color scheme: Ir (green), Au (orange), S (yellow), P (purple), O (red), N (blue), C (gray).

by slow evaporation of a CH_2Cl_2/MeOH solution. Yield: 42 mg, 62%. Anal. Calcd (%) for **2b** ($C_{31}H_{26}IrN_2S_3F_3O_5$): C, 43.70; H, 3.05; N, 3.29. Found: C, 43.44; H, 3.10; N, 3.23. ^{1}H NMR (500 MHz, CD_3CN) δ 9.18 (d, $^3J_{H2-H1}$ = 6.0 Hz, 1H, H_1), 8.37 (m, 1H, H_9), 8.22 (d, $^3J_{H3-H4}$ = 8.3 Hz, 1H, H_4), 8.12 (dd, $^3J_{H4-H3}$ = 8.3 Hz, $^3J_{H2-H3}$ = 7.5 Hz, 1H, H_3), 8.06 (m, 1H, H_{10}), 7.86 (d, $^3J_{H6-H5}$ = 7.9 Hz, 1H, H_5), 7.38 (dd, $^3J_{H3-H2}$ = 7.5 Hz, $^3J_{H1-H2}$ = 6.0 Hz, 1H, H_2), 7.17 (t, $^3J_{H5-H6}$ =$^3J_{H7-H6}$ = 7.6 Hz, 1H, H_6), 7.01 (t, $^3J_{H6-H7}$ = $^3J_{H8-H7}$ = 7.6 Hz, 1H, H_7), 6.13 (d, $^3J_{H7-H8}$ = 7.6 Hz, 1H, H_8), 2.53 (s, 3H, H_{Me}). ESI-MS: m/z 703.0 $[M\text{-}OTf]^+$.

*[Ir(ppy)$_2$(Benzene-1-(Et$_3$PAu)thiolate-2-thioether)](OTf) (**3**).* Et_3PAuCl (35 mg, 0.1 mmol) was mixed with AgOTf (26 mg, 0.1 mmol) in MeCN (30 mL) for 2 h. The colorless solution obtained was filtered and transferred to a flask containing **1a** (65.7 mg, 0.10 mmol) in MeOH (30 mL). The solution turned pale yellow after it stirred overnight. Rotoevaporation of the solvent gave yellow solids. Slow diffusion of Et_2O into a MeOH solution of the solids afforded pale yellow single crystals used for X-ray diffraction. Yield: 93 mg, 83%. Anal. Calcd (%) for **3** ($C_{36}H_{38}IrAuN_2S_3F_3O_3P$): C, 38.61; H, 3.42; N, 2.50. Found: C, 38.60; H, 3.36; N, 2.42. ^{1}H NMR (500 MHz, CD_3CN)

DOI: 10.1021/ic502875y
Inorg. Chem. 2015, 54, 2264−2277

Table 2. Selected Bond Lengths (Å) and Angles (deg) of 1a and 1b

	1a	1b		1a	1b
Ir(1)−C(1)	2.031(4)	2.012(6)	S(1)−C(23)	1.756(5)	1.806(6)
Ir(1)−C(12)	2.039(4)	2.061(6)	S(2)−C(28)	1.785(4)	1.791(6)
Ir(1)−N(1)	2.055(4)	2.061(5)	S(2)−C(29)	1.792(4)	1.792(6)
Ir(1)−N(2)	2.038(3)	2.068(5)	S(1)−O(1)		1.474(4)
Ir(1)−S(1)	2.4136(11)	2.351(2)	S(1)−O(2)		1.478(4)
Ir(1)−S(2)	2.3782(11)	2.390(2)			
C(1)−Ir(1)−N(1)	79.91(16)	80.8(2)	Ir(1)−S(2)−C(29)	111.78(16)	110.4(2)
C(12)−Ir(1)−N(2)	80.41(16)	79.7(2)	C(28)−S(2)−C(29)	102.8(2)	103.0(3)
S(1)−Ir(1)−S(2)	84.89(4)	84.73(5)	Ir(1)−S(1)−O(1)		117.51(17)
C(1)−Ir(1)−S(1)	92.88(12)	92.88(15)	Ir(1)−S(1)−O(2)		114.97(18)
C(12)−Ir(1)−S(2)	92.51(12)	93.84(15)	O(1)−S(1)−O(2)		111.8(2)
N(1)−Ir(1)−N(2)	173.03(13)	171.45(18)	C(23)−S(1)−O(1)		104.1(2)
Ir(1)−S(1)−C(23)	103.43(16)	102.85(18)	C(23)−S(1)−O(2)		103.4(2)
Ir(1)−S(2)−C(28)	104.92(16)	103.42(19)			

Table 3. Selected Bond Lengths (Å) and Angles (deg) of 2a and 2b

	2a	2b		2a	2b
Ir(1)−C(1)	2.039(4)	2.049(4)	S(1)−C(23)	1.791(4)	1.796(5)
Ir(1)−C(12)	2.029(4)	2.042(4)	S(2)−C(28)	1.779(4)	1.786(4)
Ir(1)−N(1)	2.060(3)	2.073(3)	S(1)−C(29)	1.819(4)	1.773(4)
Ir(1)−N(2)	2.060(3)	2.063(3)	S(2)−C(30)	1.805(4)	1.787(5)
Ir(1)−S(1)	2.4128(10)	2.3361(11)	S(1)−O(1)		1.463(3)
Ir(1)−S(2)	2.3907(9)	2.3397(11)	S(2)−O(2)		1.473(3)
C(1)−Ir(1)−N(1)	80.22(14)	79.47(15)	Ir(1)−S(2)−C(28)	105.05(14)	105.97(15)
C(12)−Ir(1)−N(2)	80.15(15)	80.60(15)	Ir(1)−S(2)−C(30)	109.76(15)	112.46(17)
S(1)−Ir(1)−S(2)	85.33(3)	86.31(4)	C(28)−S(2)−C(30)	101.11(19)	99.7(2)
C(1)−Ir(1)−S(1)	96.73(11)	92.11(12)	Ir(1)−S(1)−O(1)		121.83(14)
C(12)−Ir(1)−S(2)	90.70(10)	90.68(12)	C(23)−S(1)−O(1)		108.3(2)
N(1)−Ir(1)−N(2)	169.50(13)	168.12(13)	C(29)−S(1)−O(1)		107.2(2)
Ir(1)−S(1)−C(23)	103.83(14)	105.05(16)	Ir(1)−S(2)−O(2)		121.30(14)
Ir(1)−S(1)−C(29)	109.99(15)	112.83(15)	C(28)−S(2)−O(2)		108.0(2)
C(23)−S(1)−C(29)	99.32(19)	99.1(2)	C(30)−S(2)−O(2)		107.2(2)

δ 9.25 (d, $^3J_{H2-H1(H2'-H1')}$ = 5.5 Hz, 1H, $H_{1(1')}$), 8.74 (d, $^3J_{H2'-H1'(H2-H1)}$ = 5.6 Hz, 1H, $H_{1'(1)}$), 8.10−8.13 (2H, H_4, $H_{4'}$), 7.97−8.00 (2H, H_3, $H_{3'}$), 7.77 (d, $^3J_{H6-H5(H6'-H5')}$ = 7.7 Hz, 1H, $H_{5(5')}$), 7.72−7.74 (3H, $H_{5'(5)}$, H_9, H_{12}), 7.34 (dd, $^3J_{H3-H2(H3'-H2')}$ = 7.3 Hz, $^3J_{H1-H2(H1'-H2')}$ = 5.5 Hz, 1H, $H_{2(2')}$), 7.21−7.29 (3H, $H_{2'(2)}$, H_{10}, H_{11}), 7.00 (t, $^3J_{H5-H6(H5'-H6')}$ = $^3J_{H7-H6(H7'-H6')}$ = 7.7 Hz, 1H, $H_{6(6')}$), 6.96 (t, $^3J_{H5'-H6'(H5-H6)}$ = $^3J_{H7'-H6'(H7-H6)}$ = 8.4 Hz, 1H, $H_{6'(6)}$), 6.88 (t, $^3J_{H6-H7(H6'-H7')}$ = $^3J_{H8-H7(H8'-H7')}$ = 7.7 Hz, 1H, $H_{7(7')}$), 6.82 (t, $^3J_{H8'-H7'(H8-H7)}$ = $^3J_{H6'-H7'(H6-H7)}$ = 8.4 Hz, 1H, $H_{7'(7)}$), 6.35 (d, $^3J_{H7-H8(H7'-H8')}$ = 7.7 Hz, 1H, $H_{8(8')}$), 6.22 (d, $^3J_{H7'-H8'(H7-H8)}$ = 8.4 Hz, 1H, $H_{8'(8)}$), 1.71 (s, 3H, H_{Me}), 1.66 (m, 6H, H_{Et}), 0.90 (m, 9H, H_{Et}). $^{31}P\{^1H\}$ NMR (202.4 MHz, CD_3CN): δ 42.18 (s). ESI-MS: m/z 971.1 $[M\text{-}OTf]^+$.

*[Ir(ppy)$_2$(Benzene-1,2-bis((Ph$_3$PAu)thiolate)](OTf) (**4**).* Ph_3PAuCl (99 mg, 0.2 mmol) was stirred with AgOTf (52 mg, 0.2 mmol) in MeCN (30 mL) for 2 h. The mixture was filtered, and the colorless solution obtained was transferred to a Schlenk flask containing a Na[**IrSS**] (0.1 mmol) solution. The mixture was then stirred for 12 h, and a pale yellow solution resulted. Yellow solids obtained by rotoevaporation were washed several times with H_2O/MeOH (1:1). Slow diffusion of Et_2O into a CH_2Cl_2 solution of the complex afforded greenish-yellow needlelike crystals. Yield: 114 mg, 67%. Anal. Calcd (%) for **4** ($C_{65}H_{50}IrAu_2F_3N_2O_3P_2S_3$): C, 45.70; H, 2.95; N, 1.64. Found: C, 45.39; H, 3.03; N, 1.58. ^1H NMR (500 MHz, CD_3CN) δ 9.25 (d, $^3J_{H2-H1}$ = 5.3 Hz, 1H, H_1), 7.78 (m, 1H, H_9), 7.62 (t, $^3J_{Hmeta-Hpara}$ = 7.5 Hz, 3H, $H_{para-Ph3P}$), 7.52 (t, $^3J_{Hortho-Hmeta}$ = $^3J_{Hpara-Hmeta}$ = 7.5 Hz, 6H, $H_{meta-Ph3P}$), 7.44−7.47 (2H, H_4, H_5), 7.31 (t, $^3J_{H2-H3}$ = $^3J_{H4-H3}$ = 7.7 Hz, 1H, H_3), 7.21 (m, 6H, $H_{ortho-Ph3P}$), 7.08 (dd, $^3J_{H3-H2}$ = 7.3 Hz, $^3J_{H1-H2}$ = 5.3 Hz, 1H, H_2), 7.03 (m, 1H, H_{10}), 6.93 (t, $^3J_{H5-H6}$ = $^3J_{H7-H6}$ = 7.2 Hz, 1H, H_6), 6.76 (t, $^3J_{H8-H7}$ = $^3J_{H6-H7}$ = 7.2 Hz, 1H, H_7), 6.23 (d, $^3J_{H7-H8}$ = 7.2 Hz, 1H, H_8). $^{31}P\{^1H\}$ NMR (202.4 MHz, CD_3CN) δ 38.97 (s). ESI-MS: m/z 1559.2 $[M\text{-}OTf]^+$.

X-ray Crystallography. Single-crystal X-ray diffraction was carried out on a Bruker AXS SMART CCD three-circle diffractometer with a sealed tube at 223 K using graphite-monochromated Mo Kα radiation (λ = 0.710 73 Å). The software used was as follows: SMART[17] for collecting frames of data, indexing reflections, and determining lattice parameters; SAINT[17] for integration of intensity of reflections and scaling; SADABS[18] for empirical absorption correction; SHELXTL[19] for space group determination, structure solution, and least-squares refinements on $|F|^2$. Anisotropic thermal parameters were refined for the rest of the non-hydrogen atoms. The hydrogen atoms were placed in their ideal positions. Solvent molecules were found in crystal structures of **2a**·CH_3CN, **2b**·CH_3OH, and **4**·CH_2Cl_2. The triflate anion and MeOH molecule in crystal structure of **2b** are disordered over two positions with occupancies of 68:32 and 67:33, respectively. Restraints in bond lengths and thermal parameters were applied to those disordered atoms. The crystal data are summarized in Table 1.

Computational Details. Gas-phase structures of all complexes were optimized by the DFT method using B3PW91[20] hybrid functional. The 6-31G(d)[21] basis set was used for all atoms except iridium and gold, for which Stuttgart-Dresden (SDD)[22] relativistic effective core potential and associated basis sets were employed. Unrestricted formalism (UB3PW91) was used with the same basis sets for optimization of the lowest-lying triplet states. Frequency calculation was performed for all optimized geometries to ensure that the stationary point was minimum. Single-point and time-dependent (TD) DFT calculations were performed at the same functional, and basis sets with acetonitrile solvent effect described by polarizable continuum

DOI: 10.1021/ic502875y
Inorg. Chem. 2015, 54, 2264−2277

Table 4. Selected Bond Lengths (Å) and Angles (deg) of 3 and 4

	3	4		3	4
Ir(1)−C(1)	2.017(4)	2.030(4)	S(2)−C(35)	1.812(5)	
Ir(1)−C(12)	2.030(4)	2.030(5)	Au(1)−S(1)	2.3420(10)	2.322(2)
Ir(1)−N(1)	2.052(3)	2.058(4)	Au(1)−P(1)	2.2660(11)	2.256(2)
Ir(1)−N(2)	2.060(3)	2.059(4)	Au(2)−S(2)		2.322(2)
Ir(1)−S(1)	2.4264(10)	2.417(2)	Au(2)−P(2)		2.269(2)
Ir(1)−S(2)	2.4061(10)	2.423(2)			
C(1)−Ir(1)−N(1)	80.75(14)	80.08(16)	C(23)−S(1)−Au(1)	97.86(13)	98.97(14)
C(12)−Ir(1)−N(2)	80.33(15)	80.18(16)	Ir(1)−S(2)−C(28)	105.04(15)	104.97(15)
S(1)−Ir(1)−S(2)	85.83(3)	85.65(4)	Ir(1)−S(2)−C(35)	110.06(16)	
C(1)−Ir(1)−S(1)	90.86(11)	95.20(12)	C(28)−S(2)−C(35)	100.5(2)	
C(12)−Ir(1)−S(2)	95.54(12)	92.86(12)	Ir(1)−S(2)−Au(2)		110.66(4)
N(1)−Ir(1)−N(2)	169.84(13)	171.88(13)	C(28)−S(2)−Au(2)		106.41(14)
Ir(1)−S(1)−C(23)	104.69(14)	104.97(15)	S(1)−Au(1)−P(1)	175.48(4)	175.36(4)
Ir(1)−S(1)−Au(1)	109.86(4)	111.97(5)	S(2)−Au(2)−P(2)		174.97(4)

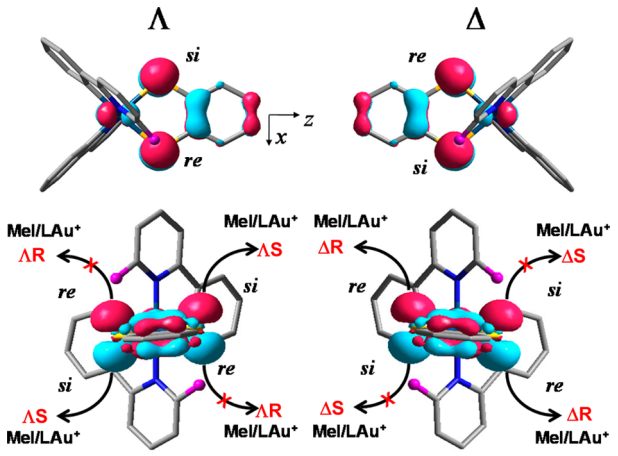

Figure 3. HOMO orbital orientation and ppy ligand steric effects as controlling factors for disastereoselectivity. (For clarity, only selected hydrogen atoms (pink) are shown).

model. Tight self-consistent field (SCF) convergence criteria were used for all calculations. Emission energy was estimated by ΔSCF approach as the difference between energies of the triplet excited state and the ground singlet state at triplet state optimized geometry.[23] All DFT calculations were performed using Gaussian 09 software package (Revision A.02).[24] Molecular orbital compositions in term of fragmental contributions were analyzed with AOMix program.[25] Frontier orbital surfaces, spin density plots, and theoretical absorption spectra were obtained using GaussView 5.0 software.

RESULTS AND DISCUSSION

Synthesis and Structures. Na[**IrSS**], which was generated in situ by reacting $Ir(ppy)_2(MeCN)_2^+$ and sodium benzene-1,2-dithiolate, reacted with 1 mol equiv of methyl iodide to produce the neutral complex **1a** [**Ir(S)(SMe)**] in 5 h. We have recently reported the DFT optimized structure, NMR, ESI-MS, absorption and emission spectroscopy (Supporting Information, Figure S1−S3) of $^nBu_4N$[**IrSS**].[12]

Darensbourg et al. showed that methylation of a Ni(II)-dithiolate complex made it less reactive toward oxygenation.[26] Similarly, we found that **1a** is much more air-stable than [**IrSS**]$^-$ as it takes more than three weeks for air to oxidize a 1×10^{-3} M solution of **1a** to the sulfinate complex **1b** [**Ir(SMe)(SO_2)**]. The oxidation is accompanied by a color change from yellow to pale yellow. The dioxygenation can be completed in 5 h using excess aqueous (aq) H_2O_2. However, excess aq H_2O_2 cannot fully oxidize **1a** to the sulfoxide−sulfinate complex **1c** [**Ir(O═SMe)(SO_2)**], whose formation requires the stronger oxidizing agent *m*-CPBA. Reacting two mol equiv of MeI with [**IrSS**]$^-$ results in the cationic dithiother complex **2a** [**Ir(SMe)(SMe)**]$^+$. As expected, **2a** is less prone to oxygenation: it is resistant to H_2O_2 and is only converted to the disulfoxide complex **2b** [**Ir(O═SMe)(O═SMe)**]$^+$ when treated with excess *m*-CPBA.

[**IrSS**]$^-$ can act as a metalloligand in complexing Ph_3PAu^+ to form the trimetallic complex **4**. Similarly, **1a** forms bimetallic complex **3** readily with Et_3PAu^+. Both **3** and **4** are air-stable and unreactive toward H_2O_2. In the presence of excess *m*-CPBA, complex **3** is oxidized to form **1c**, but **4** decomposes into a dark precipitate.

The ^{1}H NMR spectra of **1a**, **1b**, **1c**, and **3** all show two sets of eight signals for the two ppy ligands, four signals for the phenyl-S_2 rings, and a singlet for the CH_3 protons (see Figures S4−S12 for two-dimensional (2D) COSY and $^{31}P\{^1H\}$ NMR spectra

Scheme 5

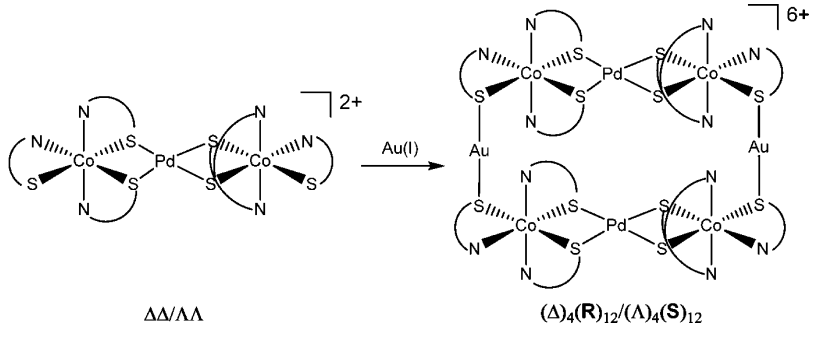

DOI: 10.1021/ic502875y
Inorg. Chem. 2015, 54, 2264−2277

in Supporting Information), which are in accord with the unsymmetrical C_i structures of the molecules verified by X-ray crystallography (vide infra). On the other hand, the ^{1}H NMR spectra of **2a** and **2b** show that the two ppy ligands in the complexes are equivalent as the spectra display only one set of eight signals for the two ppy, two signals for the S_2-phenyl ring, and one signal for methyl protons. The complex **4** has a similar ^{1}H NMR spectrum, and its ^{31}P{^{1}H} spectrum shows only one singlet at δ 38.97 ppm. The results indicate that **2a**, **2b**, and **4** have C_2 symmetry. Despite possible formation of diastereomers, which should have different NMR spectra, the spectra of the crude products of all the reactions indicate the presence of only one pair of enantiomers. In other words, the methylation and metalation are 100% diastereoselective. While it is not possible to deduce the absolute configurations of **1a**, **1b**, **1c**, and **3** from their ^{1}H NMR spectra, the spectra of **2a**, **2b**, and **4** imply that the complexes have C_2 symmetry, and hence the configurations must be either ΛRR and ΔSS or ΛSS and ΔRR.

The absolute configurations of the complexes are established by their X-ray crystal structures, which are depicted in Figure 2a–f (see Tables 2–4 for selected bond lengths and angles). Although we failed to obtain the crystal structure of **1c**, the proposed molecular structure (Scheme 3) is supported by NMR spectroscopy and high-resolution ESI-MS (Supporting Information, Figure S13).

Crystals of **1a** and **2a**, which crystallize in the non-centrosymmetric space groups $P2_12_12_1$ and $P2_1$, are enantiopure, containing the enantiomers ΔR and ΛSS, respectively. The crystals of **1b** contain both ΛS and ΔR enantiomers in their unit cells, and the enantiomers ΛSS and ΔRR are found in the crystals of **2b**, **3**, and **4**. The fact that **2a** and **2b** have the same absolute configuration indicates that oxygenation of the thioether does not alter its absolute configuration. It is therefore reasonable to assume that **1c** shares the same absolute configuration with its parental complex **1a**. The structures of the complexes indicate that the chirality around the Ir ion (Λ or Δ) dictates the absolute configuration of the chiral S atoms, as the Λ and Δ isomers react with the electrophiles to form only S and R products, respectively.

All the complexes display distorted octahedral geometry in which the central Ir ion forms five-membered rings with two orthogonal ppy ligands and an S_2-ligand. The latter forms slightly puckered IrS_2C_2 rings with IrS_2–S_2C_2 dihedral angle of 6.41°–27.64°, resulting from pyramidalization of the S atoms caused by the additions.

Despite their different electronic structures, the Ir–S(Me) bonds in four thioether-coordinated complexes **1a**, **1b**, **2a**, and **3** have similar lengths (2.3782(11)–2.4128(10) Å) and are close to the Ir–S(Me) bond distance reported for [Ir(ppy)$_2$(benzene-1-thioether-2-diphenylphosphine)] (2.4226(6) Å).[27] On the other hand, the Ir–S(Au) bonds in **3** and **4** (2.417(2)–2.4264(10) Å) are slightly longer than the Ir–S(Me) bonds (average 2.395 Å). Oxygenation of the thioether shortens the Ir–S bond as shown by Ir–S(=OMe) bond distances (2.3361(11) and 2.3397(11) Å) in **2b**. It can be accounted for by considering the decrease in atomic radius of the S atom brought about by oxidation from S(II) to S(IV). Similarly, the Ir–S(thiolate) bond in **1a** (2.4136(11) Å) is shorter than the Ir–S(O_2) bond in **1b** (2.351(2) Å), which is close to the Ir–S(O_2) bond distances observed in the crystal structure of [**IrSO$_2$SO$_2$**]$^-$ (2.348(2) and 2.352(3) Å).[12]

The O=S bond lengths and stretching frequencies (1019 and 1149 cm^{-1}) and O=S=O angle of the coordinated sulfinate in

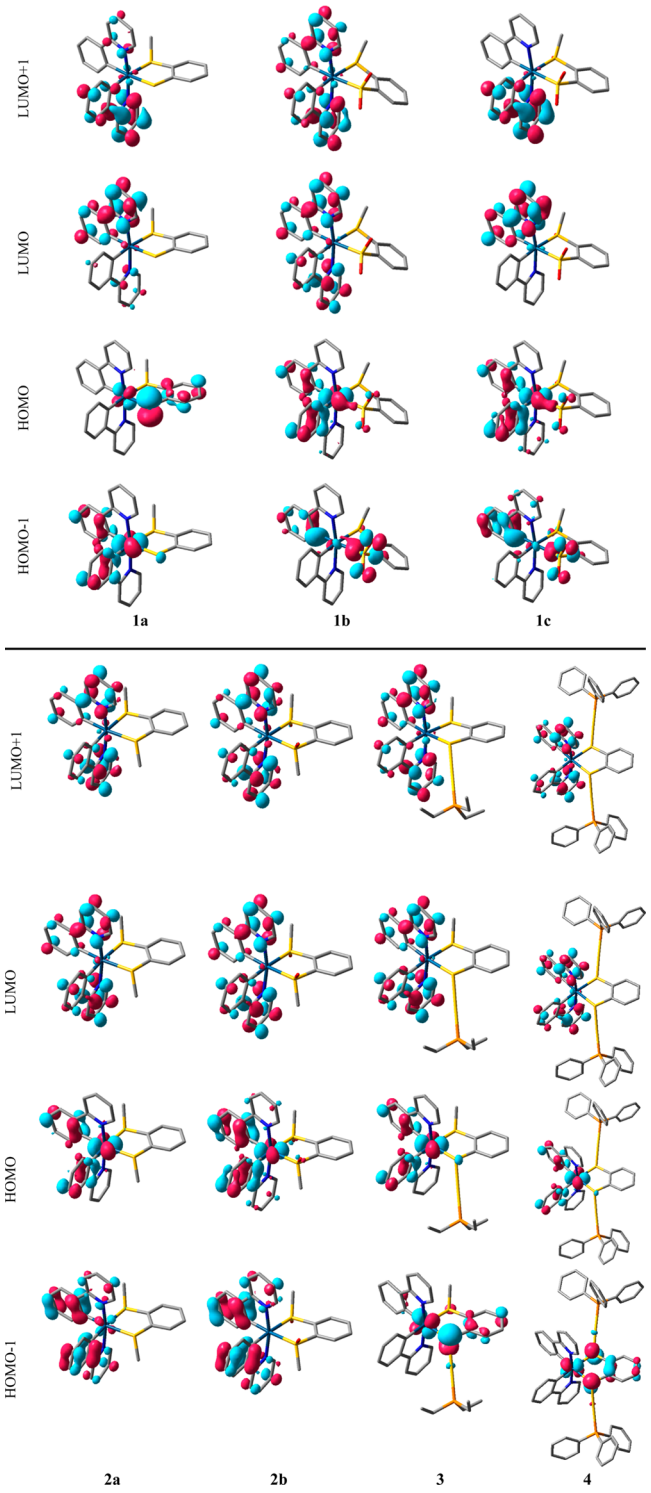

Figure 4. Frontier molecular orbital surfaces of the complexes at the ground-state optimized geometries (surface isovalue 0.05; hydrogen atoms omitted for clarity).

1b are similar to those of [**IrSO$_2$SO$_2$**]$^-$ (1014 and 1149 cm^{-1})[12] and related metal sulfinates (989–1202 cm^{-1}).[28] The O=S distances (1.463(3) and 1.473(3) Å), ν(O=S) (1106 cm^{-1}), and O=S–CH_3 angles (107.2(2)° and 107.2(2)°) in **2b** compare favorably with those in Ir^{III}(dimethyl sulfoxide) complexes such as [$IrCl_4$(H-adenine)(DMSO)][29] and [$IrCl_4$(DMSO)$_2$]$^-$[30] (DMSO = dimethyl sulfoxide) and related ruthenium complexes.[31] The infrared spectrum of **1c** displays bands ascribable to

DOI: 10.1021/ic502875y
Inorg. Chem. 2015, 54, 2264–2277

Table 5. DFT-Calculated (B3PW91/(6-31G(d)+SDD)) Energies and Compositions of HOMO−1, HOMO, LUMO, and LUMO+1 of 1a, 1b, 1c, 2a, 2b, 3, and 4

		MO composition (%)								
orbital	energy (eV)	Ir (s, p)	Ir (d)	Au	ppy (*trans* to SMe)	ppy	S(SMe)	S	O	Ph(PhSS)
					1a					
LUMO+1	−1.60	0.83	3.18		77.44	17.39	0.19	0.82		0.10
LUMO	−1.68	1.49	2.31		17.08	78.07	0.37	0.19		0.27
HOMO	−5.15	0.61	15.77		1.47	2.47	1.03	51.50		26.59
HOMO−1	−5.56	0.44	36.54		29.93	24.93	1.93	4.80		1.26
					1b					
LUMO+1	−1.72	1.37	2.93		52.71	41.58	0.41	0.35	0.29	0.24
LUMO	−1.75	1.79	2.08		42.19	52.64	0.37	0.27	0.13	0.34
HOMO	−5.76	0.32	31.67		34.83	25.01	2.23	1.56	3.72	0.44
HOMO−1	−6.15	3.70	2.93		5.82	36.88	2.94	10.02	27.90	9.56
					1c					
LUMO+1	−1.79	1.44	1.98		92.93	1.86	0.36	0.45	0.58	0.39
LUMO	−1.83	2.21	2.10		1.56	92.86	0.19	0.16	0.18	0.35
HOMO	−6.00	0.32	23.09		38.93	27.48	0.54	2.54	6.36	0.60
HOMO−1	−6.30	2.69	2.36		8.71	49.70	1.31	6.84	21.12	7.00
					2a					
LUMO+1	−1.93	1.64	2.81		93.41		0.72			0.78
LUMO	−1.99	1.94	2.11		94.78		0.61			0.39
HOMO	−6.04	0.36	31.80		62.18		3.96			1.26
HOMO−1	−6.54	0.28	5.70		89.01		3.90			0.55
					2b					
LUMO+1	−2.10	2.47	2.51		88.37		1.74		0.69	3.96
LUMO	−2.13	2.32	1.65		93.93		0.72		0.03	0.95
HOMO	−6.40	0.34	20.6		74.65		1.36		1.94	0.24
HOMO−1	−6.69	0.19	1.48		96.25		0.73		0.71	0.48
					3					
LUMO+1	−1.81	1.14	3.24	1.00	43.35	50.24	0.32	0.29		0.06
LUMO	−1.90	1.87	2.00	0.53	49.98	44.45	0.26	0.32		0.41
HOMO	−5.87	0.30	34.19	0.56	30.24	26.78	1.47	4.28		1.87
HOMO−1	−6.15	0.00	26.34	6.85	4.40	9.34	3.84	26.90		19.83
					4					
LUMO+1	−1.72	1.02	3.20	2.48		90.65		0.66		0.10
LUMO	−1.81	1.85	2.01	1.09		93.36		0.54		0.34
HOMO	−5.73	0.31	36.30	0.86		54.39		5.88		1.92
HOMO−1	−5.82	0.00	21.9	8.84		7.55		36.54		23.29

vibrations of the O═S bonds of the sulfinate (1019 and 1155 cm^{-1}) and sulfoxide (1108 cm^{-1}).

The methylated or aurated S atoms show distorted pyramidal geometry. For example, **1a**, **1b**, **2a**, **2b**, and **3** show Ir−S−C(Me) angles of 109.76(15)−112.83(15)°, which are close to the Ir−S−Au angles of 109.86(4)−111.97(5)° in **3** and **4**. The S−C(Me) distances (1.773(4)−1.819(4) Å) are typical for sulfoxides and thioethers.[9b,31] The S−Au−P angles in **3** and **4** are close to linear, as expected for the Au^{I} ion. The Au−P distances (2.256(2)−2.269(2) Å) are also similar to those of Et_3PAuCl (2.232(9) Å)[32] and Ph_3PAuCl (2.229(2) Å).[33] The S−Au bonds (2.3420(10) Å in **3** and 2.322(2) Å in **4**) are comparable with those in Au-thioether complexes such as $[Ph_3PAu(SMe_2)]$ (2.3228(12) Å)[34] and close to those in metalloligated Au complexes (2.333(7)−2.3614(12)Å)[35] such as $[(Ph_3P)_4Pt_2(\mu\text{-}S)(\mu\text{-}SAuPPh_3)]$ (2.338(2) Å).[35b] Similar to the other complexes, the DFT-optimized structure of **1c** (Supporting Information, Figure S14 and Table S1) shows a puckered IrS_2C_2 ring with IrS_2−S_2C_2 dihedral angle of 19.31°.

Stereoelectronically Controlled Diastereoselectivity. Darensbourg et al. demonstrated that dimethylation of an achiral Ni-dithiolato complex led to two pairs of disatereisomers, namely, RR and SS and RS and SR.[36] Conversely, our results show that the absolute configuration of the Ir ion (Λ or Δ) dictates the absolute configuration (R or S) of the methylated or aurated S atoms. Our previous DFT calculations showed that the optimized structure of $[\mathbf{IrSS}]^-$ has C_2 symmetry (Figure 1).[12] The lowest unoccupied molecular orbital (LUMO) is a π^* orbital of the ppy ligands, and the b_2-symmetry highest occupied molecular orbital (HOMO) is an antibonding π^* orbital arising from the interactions of the filled $3p_y$ orbitals of the two thiolate S atoms (56.8%) with the filled $5d_{yz}$ orbital of the Ir^{3+} ion (11.95%) (Figure 4) and is perpendicular to the C_2 axis. Viewing along the *y*-axis shows that for the Λ isomer, the lobes of the $3p_y$ components (the lone pairs of the S atoms) in the HOMO on the *re* faces of both S atoms are blocked by the *ortho*-H atoms of the pyridyl rings, whereas the lone pairs on the *si* faces are fully exposed (Figure 3). Conversely, for the Δ isomer, the lobes of the $3p_y$ orbitals on the *re* faces are exposed, but the ones on the *si* faces are obstructed (Figure 3). Because of the steric hindrance, the lone pairs in the Λ isomer can approach the electrophile (MeI or Ph_3PAu^+) from the *si* faces, leading to the ΛS product exclusively. The Δ isomer gives only ΔR product for the same reason.

DOI: 10.1021/ic502875y
Inorg. Chem. 2015, 54, 2264−2277

The diastereoselectivity observed is a kinetic discrimination arising from a combination of the steric effect of the ppy ligands and the orientation and nature of the HOMO, which is therefore a *stereoelectronic* effect. Stereoelectronic effects are common in organic reactions, but to date, fewer than 10 examples have been demonstrated in inorganic or organometallic reactions.[37] Our result shows that filled dπ−pπ interactions in a trisbidentate dithiolate complex give rise to a HOMO that has its *si* or *re* face sterically hindered by the two auxiliary ligands. Konno et al. reported the formation of a novel chiral octanuclear $[Au_2\{[Pd\{Co(aet)_3\}_2]\}_2]^{6+}$ (aet = 2-aminoethanethiolate) from coordination of the thiolate S atoms of $[Pd\{Co(aet)_3\}_2]^{2+}$ to Au(I) ions (Scheme 5).[6] They have shown that their reaction is diastereoselective, producing only the $(\Delta)_4(R)_{12}$ and $(\Lambda)_4(S)_{12}$ isomers.

The diastereoselectivity is the same as that exhibited in the nucleophilic addition of $[\mathbf{IrSS}]^-$. Given the fact that low-spin d^6 Co(III) in the complexes are "t_{2g}-rich", the HOMO of $[Pd\{Co(aet)_3\}_2]^{2+}$ should be a π^* orbital arising from the filled dπ−pπ antibonding interaction, similar to the HOMO in $[\mathbf{IrSSO_2}]^-$ or **1a** (vide infra).[12] We believe that the diastereoselectivity observed by Konno can be accounted for by the same stereoelectronic effect proposed in this study.

Electronic Structures. DFT calculations (B3PW91/6-31G(d)+SDD) give the nature of the frontier orbitals (HOMO−1, HOMO, LUMO, and LUMO+1) of the complexes (Figure 4). The compositions of the orbitals are shown in Table 5. The HOMO−1 of **1a** mostly comes from the π-bonding orbital of the ppy ligands and the 5d orbitals of the Ir ion. On the other hand, the HOMO is an antibonding orbital arising from interactions between the filled 3p orbital of the thiolate S atom (51.50%) and a filled dπ orbital (15.77%) of the metal (filled dπ−pπ interaction). The thiolate−sulfinate complex $[\mathbf{IrSSO_2}]^-$ (Scheme 2) reported in our previous study has a similar HOMO (3p of S (50.20%) and dπ of Ir (18.33%)).[12] The LUMO and LUMO+1 are predominantly π^* orbitals of the ppy ligand. Methylation or auration of the thiolate S removes the high-lying 3p lone pair, leading to completely different HOMOs in **1b**, **1c**, **2a**, **2b**, **3**, and **4**, which are mainly composed of the 5d orbitals of Ir and ppy π orbitals. The Au atoms have negligible contributions to the HOMOs in **3** and **4**. The LUMO and LUMO+1 orbitals of the complexes are composed mainly of ppy π^* orbitals. Notably, the HOMOs and LUMOs of the complexes resemble those of heteroleptic $[Ir(ppy)_2(acac)]$[38] and related complexes.[39] The HOMO−1 orbitals of **1b**, **1c**, **2a**, and **2b** are ppy π orbitals, but those of the aurated complexes **3** and **4** are antibonding orbitals arising from the overlap of a dπ orbital and the remaining lone pair(s) on the S atoms.

Figure 5 shows the energies of the frontier orbitals. The methylation, auration, or oxygenation does not affect the energies of LUMO and LUMO+1 significantly, as the largest difference is only 0.45 eV, observed between **1a** and **2b**. In general, the LUMOs of the neutral **1a**, **1b**, and **1c** are higher in energy than those of the cationic complexes, indicating that stabilization of the orbitals observed in the latter is mainly due to an increase in Coulombic attraction.

The HOMO of **1a** is much higher in energy than the HOMOs of the other complexes because of its antibonding nature. The energies of the HOMOs in the rest of the complexes vary at most by 0.7 eV. Methylation and auration of the S atoms lowers the energy of the HOMO with the former having a stronger effect than the latter. For instance, the HOMO of the dimethylated **2a** is 0.31 eV lower than that of the diaurated **4**. Oxygenation can further stabilize the HOMO as

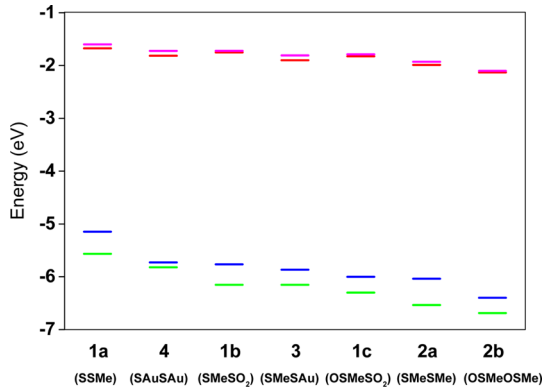

Figure 5. Plot of the frontier orbital energies of the complexes in order of descending HOMO energies. HOMO−1 (green), HOMO (blue), LUMO (red), and LUMO+1 (magenta).

shown by the HOMO of **2b**, which is 0.36 eV lower than that of **2a**. As the energy of the HOMO of all the complexes except **1a** depends primarily on the σ-donating strength of the S_2-ligands, the ligand field strength of the neutral ligands can be arranged in the order of diauratedithiolate > dithioether > disulfoxide.

Electronic Spectroscopy. UV−vis absorption spectra of CH_3CN solutions of the complexes are shown in Figure 6, and the spectroscopic and photophysical data are listed in Table 6. TD-DFT calculations predict the energies and oscillator strengths

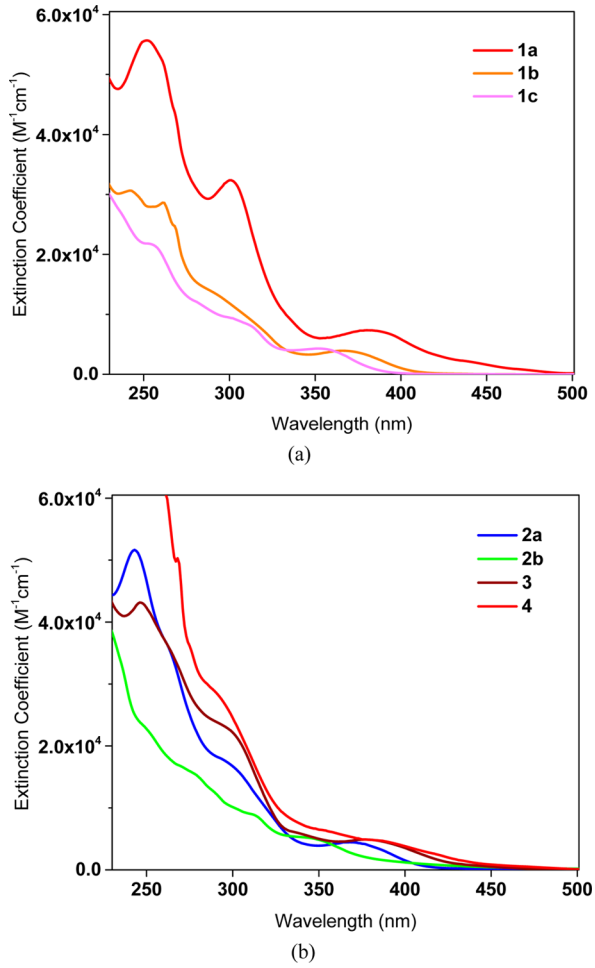

Figure 6. UV−vis absorption spectra of (a) **1a**, **1b**, and **1c** and (b) **2a**, **2b**, **3**, and **4** in CH_3CN at room temperature.

DOI: 10.1021/ic502875y
Inorg. Chem. 2015, 54, 2264−2277

Table 6. UV−vis Absorption and Emission Data

compound	absorption maxima, nm (ε, 10^3 $M^{-1}cm^{-1}$)	emission, nm	emission lifetime τ, μs	emission quantum yield Φ
1a	445 (1.87); 381 (7.35); 300 (32.38)	560	0.42	0.51
1b	365 (3.96); 290 (13.81); 261 (28.83)	496	0.56	0.20
1c	354 (4.32); 313 (8.20); 303 (9.33)	492	0.72	0.16
2a	370 (4.57); 295 (17.89); 262 (36.37)	497	0.74	0.27
2b	350 (5.08); 313 (8.97); 275 (15.88)	486	1.2	0.14
3	379 (4.83); 340 (5.83); 298 (22.67)	494	0.26	0.06
4	388 (4.82); 355 (6.46); 290 (28.83); 266 (50.33)	481	0.61	0.09

of spin-allowed electronic transitions, which are selectively shown in Table 7.

All spectra exhibit very intense high-energy absorptions ($\varepsilon > 1 \times 10^4$ $M^{-1}cm^{-1}$) at wavelength <270 nm and a shoulder at ~300 nm, which are attributed to $^1\pi \rightarrow \pi^*$ and high-energy metal-to-ligand(ppy π^*)-charge-transfer (MLCT) transitions. Another common feature is a moderately intense absorption band between 330 and 430 nm. The bands of **1a** (λ_{max} = 381 nm, $\varepsilon_{max} = 7.35 \times 10^3$ $M^{-1}cm^{-1}$) and **4** (λ_{max} = 388 nm, $\varepsilon_{max} = 4.82 \times 10^3$ $M^{-1}cm^{-1}$) are distinctly lower in energy than **2b** (λ_{max} = 350 nm, $\varepsilon_{max} = 5.08 \times 10^3$ $M^{-1}cm^{-1}$), suggesting that the transition has substantial MLCT character. Similar absorption bands are observed in the spectra of *fac*-Ir(ppy)$_3$ (λ_{max} = 376 nm, $\varepsilon_{max} = 7.20 \times 10^3$ $M^{-1}cm^{-1}$)[40] and many of its heteroleptic derivatives and are assigned to HOMO → LUMO ($^1\pi \rightarrow \pi^*$/MLCT) transitions.[14,39a,41] Indeed, TD-DFT calculations show that the bands correspond to the HOMO → LUMO transitions for **1b**, **1c**, **2a**, **2b**, **3**, and **4** and the HOMO−1 → LUMO transition for **1a**, which are $^1\pi \rightarrow \pi^*$/MLCT in nature. Only the spectrum of **1a** exhibits an absorption between 430 and 500 nm (λ_{max} = 445 nm, $\varepsilon_{max} = 1.87 \times 10^3$ $M^{-1}cm^{-1}$), which is the HOMO → LUMO transition. According to the antibonding dπ−pπ nature of the HOMO, the transition is predominantly ligand(3p of S)-to-ligand(π^* of ppy)-charge-transfer mixed with MLCT (LLCT/MLCT). Our previous study showed that the thiolate−sulfinate $[\mathbf{IrSSO_2}]^-$ (Scheme 2) displayed a LLCT/MLCT band at similar wavelength (λ_{max} = 440 nm, $\varepsilon_{max} = 1.40 \times 10^3$ M^{-1} cm^{-1}).[12] The calculated spectra reproduce the essential features of their experimental counterparts (see Figures S15−S21 in Supporting Information,).

Emission. All of the complexes are photoluminescent in degassed CH_3CN at room temperature. Figure 7 shows the emission spectra, and the emission lifetimes and quantum yields are listed in Table 6. The optimized structures of the lowest-energy triplet excited states (T_1) were obtained by unrestricted Kohn−Sham calculations (see Supporting Information, Tables S2−S4 for selected structural parameters), and the energies of T_1 obtained from ΔSCF calculations are listed in Table 8. Surface plots of the spin-density distribution of the optimized T_1 states are shown in Figure 8.

The emission lifetimes are on the order of 10^{-1} μs, indicating that the emissive excited states have substantial triplet spin parentage. Except **1a**, all of the complexes show vibronic emissions at similar energies (λ_{max} = 481−497 nm). The complex *fac*-Ir(ppy)$_3$ and its heteroleptic derivatives display similar vibronic emissions, which come from $^3\pi\pi^*$/MLCT excited states.[14,23a,39b,41c−i,42] TD-DFT calculations show that the T_1

Table 7. Selected TD-DFT (B3PW91/(6-31G(d) + SDD)) Calculated Singlet Excitation Energies of the Complexes in CH_3CN

complex	excitation energy, nm	oscillator strength	transition	contribution (%)	λ, nm (expt)	ε, 10^3 $M^{-1}cm^{-1}$ (expt)
1a	440	0.0018	H→L	98	445	1.87
	431	0.0110	H→L+1	98		
	393	0.0492	H-1→L	97	381	7.35
	301	0.0744	H-3→L+1	70	300	32.38
1b	376	0.0696	H→L	97	365	3.96
	371	0.0019	H→L+1	98		
	295	0.0564	H-3→L+1	23		
			H-1→L+3	17		
	290	0.0534	H-4→L+1	34	290	13.81
1c	355	0.0491	H→L	97	354	4.32
	352	0.0290	H→L+1	97		
	307	0.0197	H-2→L	81	313	8.20
			H→L+2	5		
	304	0.0759	H-2→L+1	80	303	9.33
2a	373	0.0618	H→L	97	370	4.57
	294	0.0838	H-4→L+1	51	295	17.89
2b	346	0.0848	H→L	97	350	5.08
	309	0.0797	H-1→L+1	93	313	8.97
3	383	0.0477	H→L	97	379	4.83
	372	0.0014	H→L+1	97	372	4.52
	348	0.0115	H-1→L	92	340	5.83
			H-1→L+1	4		
	294	0.0811	H-4→L	48	298	22.67
			H→L+4	13		
4	390	0.0373	H→L	97	388	4.82
	372	0.0004	H-1→L	90	372	5.08
	365	0.0089	H-1→L+1	96	355	6.46

DOI: 10.1021/ic502875y
Inorg. Chem. 2015, 54, 2264−2277

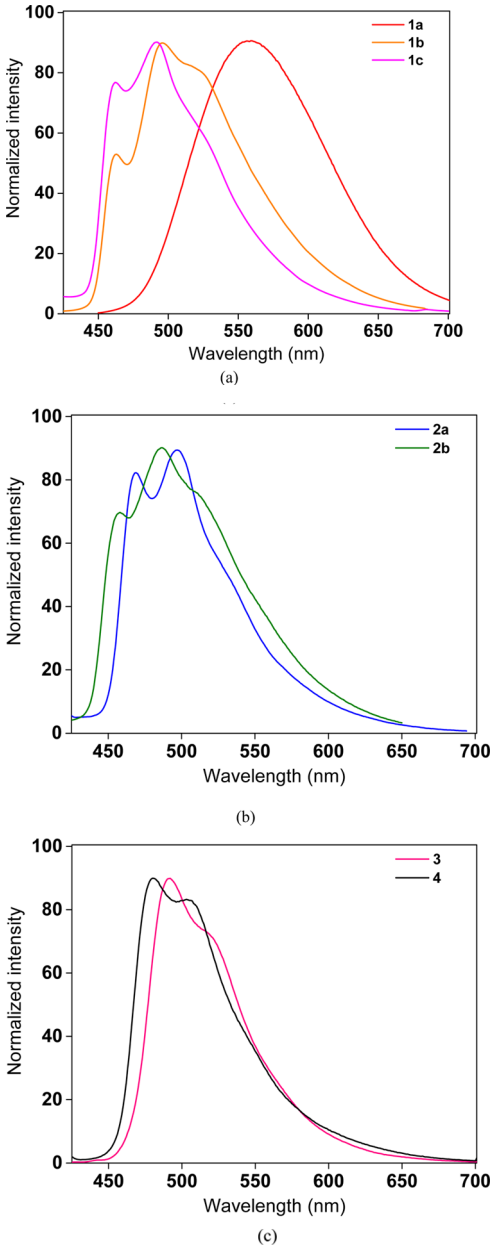

Figure 7. Normalized emission spectra of degassed CH_3CN solutions of the complexes (a) **1a**, **1b**, and **1c** and (b) **2a** and **2b**, and (c) **3** and **4** (excitation wavelength = 370 nm).

Table 8. $\Delta E(T_1 \rightarrow S_0)$ Calculated Using Lowest Excited-State Optimized Geometries Using ΔSCF Method

	emission energy, nm	
compound	experimental value	calculated value
1a	560	542
1b	496	510
1c	492	508
2a	497	515
2b	486	512
3	494	516
4	481	520

states of the complexes arise from HOMO → LUMO transitions (68−88%). Spin density on the ppy ligand and the metal ion is observed in the T_1 state (Figure 8), which is consistent with a

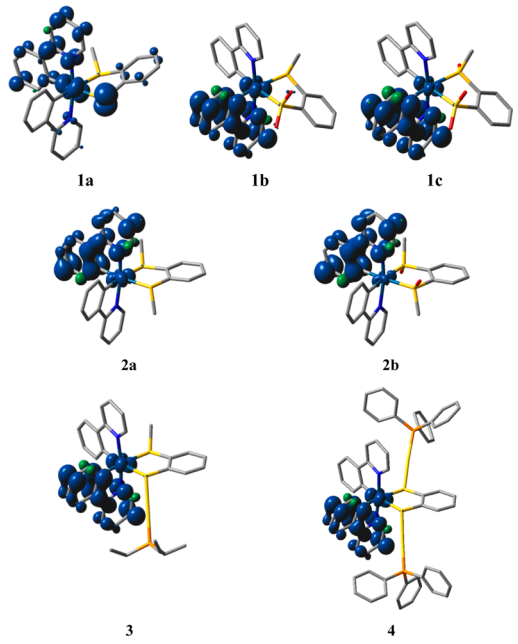

Figure 8. Plots of spin density (isovalue 0.005) of the lowest triplet excited state of **1a**, **1b**, **1c**, **2a**, **2b**, **3**, and **4**.

$\pi\pi^*$/MLCT assignment. The $T_1 \rightarrow S_0$ (singlet ground state) transition energies computed by ΔSCF methods deviate slightly from the emission maxima (Table 8). The shape of the emissions of **2a**, **3**, and **4** and the corresponding Huang−Rhys ratios S of ∼1 ($S = I_{1,0}/I_{0,0}$, where $I_{1,0}$ and $I_{0,0}$ are the intensity of the first and the second vibronic peaks, respectively) are similar to those of the ^{3}MLCT emission of $Ru(bipy)_3^{2+}$ (bipy = 2,2′-bipyridine),[43] suggesting that the excited states of the complexes possess high charge-transfer character. On the other hand, the larger S values of the emissions of **1b** (1.7), **1c** (1.2), and **2b** (1.3) suggest higher intraligand $\pi\pi^*$ weightage in the emissive excited states of the complxes.[39b]

The complex **1a** displays an intense (τ = 0.42 μs, Φ = 0.51), broad, and structureless emission at lower energy (λ_{max} = 560 nm). $[\mathbf{IrSSO_2}]^-$ displays similar emission (λ_{max} = 550 nm, τ = 0.12 μs, Φ = 0.13), which is assigned to ^{3}LLCT/MLCT.[12] Similar broad and unstructured LLCT/MLCT emissions are displayed by (bipy)Pt(benzene-1,2-dithiolate) and related complexes.[44] The calculated T_1 state of **1a** has spin densities on the lone pair of the thiolate S, the Ir ion, and the π^* orbital of a ppy ligand, indicating LLCT/MCT nature of the excited state and the phosphorescence derived from its decay. The computed energy of the $T_1 \rightarrow S_0$ transition (542 nm, 2.29 eV) is slightly higher than the emission maxima (λ_{max} = 560 nm, 2.21 eV) of the complex.

The calculation predicts a shortening of the Ir−S(thiolate) bond of **1a** in its T_1 state (2.400 vs 2.460 Å in S_0) indicating an increase in Ir−S(thiolate) bond order in the excited state. It can be accounted for by considering the formation of a partial Ir−S double bond in the excited state as the T_1 excited state is generated from promotion of an electron in the antibonding π^* orbital of the Ir−S bond (HOMO) to a π^* orbital of ppy (LUMO). The decrease in electron density in the Ir−S π^* orbital would lead to a partial π bond in addition to the existing Ir−S σ bond, leading to an increase in formal bond order.

CONCLUSION

It is demonstrated in this study that the dithiolate complex $[\mathbf{IrSS}]^-$ is a diastereoselective nucleophile and metalloligand.

DOI: 10.1021/ic502875y
Inorg. Chem. 2015, 54, 2264−2277

The diastereoselectivity is due to a stereoelectronic effect, which is a combined effect of the helical chirality of the metal complex (stereo) and the symmetry of the HOMO (electronic). The antibonding $d\pi-p\pi$ interactions, which give rise to the HOMO, are essential for the stereoelectronic effect, and it is believed that the effect can operate in trisbidentate complexes of t_{2g}-rich metals containing an auxiliary thiolate ligand. Methylation and auration of $[\mathbf{IrSS}]^-$ gives a lower-energy HOMO that is mainly composed of metal d-orbital and π-orbital of ppy. Oxygenation converts the ligands to sulfinate or sulfoxide and further stabilizes the HOMO. The absorption and emission spectroscopy of all the derivatives of the thiolate−thioether complex **1a** examined in this study is similar to the parental homoleptic *fac*-Ir(ppy)$_3$ and related compounds, showing $^3\pi\pi^*$/MLCT emission. On the other hand, the complex **1a** displays low-energy ^{1}LLCT/MLCT absorption at 445 nm and relatively intense and long-lived ^{3}LLCT/MLCT phosphorescence. It is expected that the strong nucleophilicity of $[\mathbf{IrSS}]^-$ can be harnessed to construct multichromophoric systems or to bind and activate electrophilic small molecules such as SO_2. Work in this direction is now being pursued in our laboratory.

■ ASSOCIATED CONTENT

Supporting Information

2D-COSY and $^{31}P\{^1H\}$ NMR spectra and ESI-MS of the complexes, DFT-optimized structure and selected structural parameters of **1c**, TD-DFT calculated absorption spectra, and selected structural parameters of the lowest energy triplet excited states. This material is available free of charge via the Internet at http://pubs.acs.org.

■ AUTHOR INFORMATION

Corresponding Author

*E-mail: chmyiphk@nus.edu.sg.

Notes

The authors declare no competing financial interest.

■ ACKNOWLEDGMENTS

We are grateful to Prof. K. L. Lin and Ms. T. GeokKheng for determining the X-ray structures. The Ministry of Education (R-143-000-548-112) of Singapore and the National University of Singapore are thanked for financial support.

■ REFERENCES

(1) (a) Sokolov, M. N.; Abramov, P. A. *Coord. Chem. Rev.* **2012**, *256*, 1972. (b) Briant, C. E.; Gilmour, D. I.; Luke, M. A.; Mingos, D. M. P. *J. Chem. Soc., Dalton Trans.* **1985**, 851. (c) Gilmour, D. I.; Luke, M. A.; Mingos, D. M. P. *J. Chem. Soc., Dalton Trans.* **1987**, 335. (d) Bos, W.; Bour, J. J.; Schlebos, P. P. J.; Hageman, P.; Bosman, W. P.; Smits, J. M. M.; van Wietmarschen, J. A. C.; Beurskens, P. T. *Inorg. Chim. Acta* **1986**, *119*, 141. (e) Briant, C. E.; Hor, T. S. A.; Howells, N. D.; Mingos, D. M. P. *J. Chem. Soc., Chem. Commun.* **1983**, 1118. (f) Jain, V. K.; Jain, L. *Coord. Chem. Rev.* **2005**, *249*, 3075. (g) Liu, H.; Tan, A. L.; Mok, K. F.; Mak, T. C. W.; Batsanov, A. S.; Howard, J. A. K.; Hor, T. S. A. *J. Am. Chem. Soc.* **1997**, *119*, 11006. (h) Hidai, M.; Kuwata, S.; Mizobe, Y. *Acc. Chem. Res.* **1999**, *33*, 46. (i) Jin, G.-X.; Wang, J.-Q.; Zhang, C.; Weng, L.-H.; Herberhold, M. *Angew. Chem., Int. Ed.* **2005**, *44*, 259. (j) Wang, J.-Q.; Cai, S.; Jin, G.-X.; Weng, L.-H.; Herberhold, M. *Chem.—Eur. J.* **2005**, *11*, 7342. (k) Shin, R. Y. C.; Goh, L. Y. *Acc. Chem. Res.* **2006**, *39*, 301. (l) Oji, K.; Igashira-Kamiyama, A.; Yoshinari, N.; Konno, T. *Angew. Chem., Int. Ed.* **2014**, *53*, 1992. (m) Rampersad, M. V.; Jeffery, S. P.; Reibenspies, J. H.; Ortiz, C. G.; Darensbourg, D. J.; Darensbourg, M. Y. *Angew. Chem., Int. Ed.* **2005**, *44*, 1217.

(2) (a) Buhro, W. E.; Zwick, B. D.; Georgiou, S.; Hutchinson, J. P.; Gladysz, J. A. *J. Am. Chem. Soc.* **1988**, *110*, 2427. (b) Giner Planas, J.; Hampel, F.; Gladysz, J. A. *Chem.—Eur. J.* **2005**, *11*, 1402. (c) Bohle, D. S.; Clark, G. R.; Rickard, C. E. F.; Roper, W. R. *J. Organomet. Chem.* **1990**, *393*, 243. (d) Berenguer, J. R.; Chaouche, N.; Fornies, J.; Fortuno, C.; Martin, A. *New J. Chem.* **2006**, *30*, 473. (e) Mastrorilli, P. *Eur. J. Inorg. Chem.* **2008**, *2008*, 4835.

(3) Chatt, J.; Mingos, D. M. P. *J. Chem. Soc. A* **1970**, 1243.

(4) (a) Aw, B. H.; Looh, K. K.; Chan, H. S. O.; Tan, K. L.; Hor, T. S. A. *J. Chem. Soc., Dalton Trans.* **1994**, 3177. (b) Liu, H.; Tan, A. L.; Mok, K. F.; Hor, T. S. A. *J. Chem. Soc., Dalton Trans.* **1996**, 4023. (c) Zhou, M.; Xu, Y.; Lam, C.-F.; Leung, P.-H.; Koh, L.-L.; Mok, K. F.; Hor, T. S. A. *Inorg. Chem.* **1994**, *33*, 1572.

(5) (a) Baker-Hawkes, M. J.; Dori, Z.; Eisenberg, R.; Gray, H. B. *J. Am. Chem. Soc.* **1968**, *90*, 4253. (b) Enemark, J. H.; Lipscomb, W. N. *Inorg. Chem.* **1965**, *4*, 1729. (c) Christou, G.; Huffman, J. C. *J. Chem. Soc., Chem. Commun.* **1983**, 558. (d) Hamilton, W. C.; Bernal, I. *Inorg. Chem.* **1967**, *6*, 2003. (e) Snow, M. R.; Ibers, J. A. *Inorg. Chem.* **1973**, *12*, 249. (f) Kanatzidis, M. G.; Coucouvanis, D. *Inorg. Chem.* **1984**, *23*, 403.

(6) Konno, T.; Chikamoto, Y.; Okamoto, K.-i.; Yamaguchi, T.; Ito, T.; Hirotsu, M. *Angew. Chem., Int. Ed.* **2000**, *39*, 4098.

(7) Ashby, M. T.; Enemark, J. H.; Lichtenberger, D. L. *Inorg. Chem.* **1988**, *27*, 191.

(8) (a) Hubbard, J. L.; Lichtenberger, D. L. *Inorg. Chem.* **1980**, *19*, 3865. (b) Fox, D. C.; Fiedler, A. T.; Halfen, H. L.; Brunold, T. C.; Halfen, J. A. *J. Am. Chem. Soc.* **2004**, *126*, 7627.

(9) (a) Smee, J. J.; Miller, M. L.; Grapperhaus, C. A.; Reibenspies, J. H.; Darensbourg, M. Y. *Inorg. Chem.* **2001**, *40*, 3601. (b) Farmer, P. J.; Reibenspies, J. H.; Lindahl, P. A.; Darensbourg, M. Y. *J. Am. Chem. Soc.* **1993**, *115*, 4665. (c) Grapperhaus, C. A.; Darensbourg, M. Y. *Acc. Chem. Res.* **1998**, *31*, 451.

(10) Shin, R. Y. C.; Tan, G. K.; Koh, L. L.; Vittal, J. J.; Goh, L. Y.; Webster, R. D. *Organometallics* **2005**, *24*, 539.

(11) (a) Goodman, D. C.; Tuntulani, T.; Farmer, P. J.; Darensbourg, M. Y.; Reibenspies, J. H. *Angew. Chem., Int. Ed.* **1993**, *32*, 116. (b) Almaraz, E.; Foley, W. S.; Denny, J. A.; Reibenspies, J. H.; Golden, M. L.; Darensbourg, M. Y. *Inorg. Chem.* **2009**, *48*, 5288.

(12) Nguyen, V. H.; Chew, H. Q.; Su, B.; Yip, J. H. K. *Inorg. Chem.* **2014**, *53*, 9739.

(13) Armarego, W. L. F.; Chai, C. L. L. In *Purification of Laboratory Chemicals,* 6th ed.; Butterworth-Heinemann: Oxford, U.K., 2009.

(14) Sprouse, S.; King, K. A.; Spellane, P. J.; Watts, R. J. *J. Am. Chem. Soc.* **1984**, *106*, 6647.

(15) Mann, F. G.; Wells, A. F.; Purdie, D. *J. Chem. Soc.* **1937**, 1828.

(16) Bruce, M. I.; Nicholson, B. K.; Shawkataly, O. B. *Inorg. Synth.* **1989**, *26*, 324.

(17) *SMART&SAINT software Reference Manuals;* Bruker AXS, Inc.: Madison, WI, USA, 2007.

(18) *SADABS: Software for Empirical Absorption Correction;* Bruker AXS, Inc.: Madison, WI, USA, 2001.

(19) Sheldrick, G. *Acta Crystallogr., Sect. A* **2008**, *64*, 112.

(20) (a) Becke, A. D. *J. Chem. Phys.* **1993**, *98*, 5648. (b) Perdew, J. P.; Wang, Y. *Phys. Rev. B* **1992**, *45*, 13244.

(21) (a) Hariharan, P. C.; Pople, J. A. *Theor. Chim. Acta* **1973**, *28*, 213. (b) Francl, M. M.; Pietro, W. J.; Hehre, W. J.; Binkley, J. S.; Gordon, M. S.; DeFrees, D. J.; Pople, J. A. *J. Chem. Phys.* **1982**, *77*, 3654.

(22) Andrae, D.; Häußermann, U.; Dolg, M.; Stoll, H.; Preuß, H. *Theor. Chim. Acta* **1990**, *77*, 123.

(23) (a) Avilov, I.; Minoofar, P.; Cornil, J.; De Cola, L. *J. Am. Chem. Soc.* **2007**, *129*, 8247. (b) Salassa, L.; Garino, C.; Salassa, G.; Gobetto, R.; Nervi, C. *J. Am. Chem. Soc.* **2008**, *130*, 9590. (c) Davies, D. L.; Lelj, F.; Lowe, M. P.; Ryder, K. S.; Singh, K.; Singh, S. *Dalton Trans.* **2014**, *43*, 4026.

(24) Frisch, M. J.; Trucks, G. W.; Schlegel, H. B.; Scuseria, G. E.; Robb, M. A.; Cheeseman, J. R.; Scalmani, G.; Barone, V.; Mennucci, B.; Petersson, G. A.; Nakatsuji, H.; Caricato, M.; Li, X.; Hratchian, H. P.; Izmaylov, A. F.; Bloino, J.; Zheng, G.; Sonnenberg, J. L.; Hada, M.;

DOI: 10.1021/ic502875y
Inorg. Chem. 2015, 54, 2264−2277

Ehara, M.; Toyota, K.; Fukuda, R.; Hasegawa, J.; Ishida, M.; Nakajima, T.; Honda, Y.; Kitao, O.; Nakai, H.; Vreven, T.; Montgomery, J. A., Jr.; Peralta, J. E.; Ogliaro, F.; Bearpark, M. J.; Heyd, J.; Brothers, E. N.; Kudin, K. N.; Staroverov, V. N.; Kobayashi, R.; Normand, J.; Raghavachari, K.; Rendell, A. P.; Burant, J. C.; Iyengar, S. S.; Tomasi, J.; Cossi, M.; Rega, N.; Millam, N. J.; Klene, M.; Knox, J. E.; Cross, J. B.; Bakken, V.; Adamo, C.; Jaramillo, J.; Gomperts, R.; Stratmann, R. E.; Yazyev, O.; Austin, A. J.; Cammi, R.; Pomelli, C.; Ochterski, J. W.; Martin, R. L.; Morokuma, K.; Zakrzewski, V. G.; Voth, G. A.; Salvador, P.; Dannenberg, J. J.; Dapprich, S.; Daniels, A. D.; Farkas, Ö.; Foresman, J. B.; Ortiz, J. V.; Cioslowski, J.; Fox, D. J. *Gaussian 09;* Gaussian, Inc.: Wallingford, CT, USA, 2009.

(25) (a) Gorelsky, S. I.; Lever, A. B. P. *J. Organomet. Chem.* **2001**, *635*, 187. (b) Gorelsky, S. I. *AOMix: Program for Molecular Orbital Analysis*; 2013; http://www.sg-chem.net/.

(26) Bellefeuille, J. A.; Grapperhaus, C. A.; Buonomo, R. M.; Reibenspies, J. H.; Darensbourg, M. Y. *Organometallics* **1998**, *17*, 4813.

(27) Constable, E. C.; Housecroft, C. E.; Schönhofer, E.; Schönle, J.; Zampese, J. A. *Polyhedron* **2012**, *35*, 154.

(28) (a) Tuntulani, T.; Musie, G.; Reibenspies, J. H.; Darensbourg, M. Y. *Inorg. Chem.* **1995**, *34*, 6279. (b) Begum, R. A.; Farah, A. A.; Hunter, H. N.; Lever, A. B. P. *Inorg. Chem.* **2009**, *48*, 2018.

(29) García-Raso, A.; Fiol, J. J.; Albertí, F. M.; Lagos, Y.; Torres, M.; Barceló-Oliver, M.; Prieto, M. J.; Moreno, V.; Mata, I.; Molins, E.; Estarellas, C.; Frontera, A.; Quiñonero, D.; Deyà, P. M. *Eur. J. Inorg. Chem.* **2010**, *2010*, 5617.

(30) Albertí, F. M.; Fiol, J. J.; García-Raso, A.; Torres, M.; Terrón, A.; Barceló-Oliver, M.; Prieto, M. J.; Moreno, V.; Molins, E. *Polyhedron* **2010**, *29*, 34.

(31) (a) Lai, C.-Y.; Mak, W.-L.; Chan, E. Y. Y.; Sau, Y.-K.; Zhang, Q.-F.; Lo, S. M. F.; Williams, I. D.; Leung, W.-H. *Inorg. Chem.* **2003**, *42*, 5863. (b) Yapp, D. T. T.; Rettig, S. J.; James, B. R.; Skov, K. A. *Inorg. Chem.* **1997**, *36*, 5635.

(32) Tiekink, E. R. T. *Acta Crystallogr., Sect. C: Cryst. Struct. Commun.* **1989**, *45*, 1233.

(33) Kouroulis, K. N.; Hadjikakou, S. K.; Kourkoumelis, N.; Kubicki, M.; Male, L.; Hursthouse, M.; Skoulika, S.; Metsios, A. K.; Tyurin, V. Y.; Dolganov, A. V.; Milaeva, E. R.; Hadjiliadis, N. *Dalton Trans.* **2009**, 10446.

(34) (a) Sladek, A.; Schmidbaur, H. *Z. Naturforsch., B* **1996**, *51*, 1207. (b) Banide, E. V.; Grealis, J. P.; Müller-Bunz, H.; Ortin, Y.; Casey, M.; Mendicute-Fierro, C.; Cristina Lagunas, M.; McGlinchey, M. J. *J. Organomet. Chem.* **2008**, *693*, 1759.

(35) (a) Robertson, S. D.; Slawin, A. M. Z.; Woollins, J. D. *Eur. J. Inorg. Chem.* **2007**, *2007*, 247. (b) Li, Z.; Loh, Z.-H.; Mok, K. F.; Hor, T. S. A. *Inorg. Chem.* **2000**, *39*, 5299. (c) Pinder, T. A.; Montalvo, S. K.; Lunsford, A. M.; Hsieh, C.-H.; Reibenspies, J. H.; Darensbourg, M. Y. *Dalton Trans.* **2014**, *43*, 138.

(36) Darensbourg, M. Y.; Font, I.; Mills, D. K.; Pala, M.; Reibenspies, J. H. *Inorg. Chem.* **1992**, *31*, 4965.

(37) (a) Kiel, W. A.; Lin, G. Y.; Constable, A. G.; McCormick, F. B.; Strouse, C. E.; Eisenstein, O.; Gladysz, J. A. *J. Am. Chem. Soc.* **1982**, *104*, 4865. (b) Crocco, G. L.; Gladysz, J. A. *J. Am. Chem. Soc.* **1985**, *107*, 4103. (c) Heah, P. C.; Patton, A. T.; Gladysz, J. A. *J. Am. Chem. Soc.* **1986**, *108*, 1185. (d) Bodner, G. S.; Smith, D. E.; Hatton, W. G.; Heah, P. C.; Georgiou, S.; Rheingold, A. L.; Geib, S. J.; Hutchinson, J. P.; Gladysz, J. A. *J. Am. Chem. Soc.* **1987**, *109*, 7688. (e) Smith, D. E.; Gladysz, J. A. *Organometallics* **1985**, *4*, 1480. (f) Senn, D. R.; Wong, A.; Patton, A. T.; Marsi, M.; Strouse, C. E.; Gladysz, J. A. *J. Am. Chem. Soc.* **1988**, *110*, 6096. (g) Ahmed, K. J.; Chisholm, M. H.; Huffman, J. C. *Organometallics* **1985**, *4*, 1312. (h) Calhorda, M. J.; Hoffmann, R. *Organometallics* **1986**, *5*, 2181. (i) Blackburn, B. K.; Bromley, L.; Davies, S. G.; Whittaker, M.; Jones, R. H. *J. Chem. Soc., Perkin Trans. 2* **1989**, 1143.

(38) (a) Hay, P. J. *J. Phys. Chem. A* **2002**, *106*, 1634. (b) Djurovich, P. I.; Murphy, D.; Thompson, M. E.; Hernandez, B.; Gao, R.; Hunt, P. L.; Selke, M. *Dalton Trans.* **2007**, 3763.

(39) (a) Zhang, S.; Si, Y.; Wu, Z. *RSC Adv.* **2014**, *4*, 15849. (b) Li, J.; Djurovich, P. I.; Alleyne, B. D.; Yousufuddin, M.; Ho, N. N.; Thomas, J. C.; Peters, J. C.; Bau, R.; Thompson, M. E. *Inorg. Chem.* **2005**, *44*, 1713.

(40) (a) Hofbeck, T.; Yersin, H. *Inorg. Chem.* **2010**, *49*, 9290. (b) King, K. A.; Spellane, P. J.; Watts, R. J. *J. Am. Chem. Soc.* **1985**, *107*, 1431.

(41) (a) Zhang, F.; Wang, L.; Chang, S.-H.; Huang, K.-L.; Chi, Y.; Hung, W.-Y.; Chen, C.-M.; Lee, G.-H.; Chou, P.-T. *Dalton Trans.* **2013**, *42*, 7111. (b) Li, S. P.-Y.; Tang, T. S.-M.; Yiu, K. S.-M.; Lo, K. K.-W. *Chem.—Eur. J.* **2012**, *18*, 13342. (c) Lamansky, S.; Djurovich, P.; Murphy, D.; Abdel-Razzaq, F.; Kwong, R.; Tsyba, I.; Bortz, M.; Mui, B.; Bau, R.; Thompson, M. E. *Inorg. Chem.* **2001**, *40*, 1704. (d) Colombo, M. G.; Brunold, T. C.; Riedener, T.; Guedel, H. U.; Fortsch, M.; Buergi, H.-B. *Inorg. Chem.* **1994**, *33*, 545. (e) Lamansky, S.; Djurovich, P.; Murphy, D.; Abdel-Razzaq, F.; Lee, H.-E.; Adachi, C.; Burrows, P. E.; Forrest, S. R.; Thompson, M. E. *J. Am. Chem. Soc.* **2001**, *123*, 4304. (f) Schmid, B.; Garces, F. O.; Watts, R. J. *Inorg. Chem.* **1994**, *33*, 9. (g) Orselli, E.; Kottas, G. S.; Konradsson, A. E.; Coppo, P.; Fröhlich, R.; De Cola, L.; van Dijken, A.; Büchel, M.; Börner, H. *Inorg. Chem.* **2007**, *46*, 11082. (h) Ragni, R.; Plummer, E. A.; Brunner, K.; Hofstraat, J. W.; Babudri, F.; Farinola, G. M.; Naso, F.; De Cola, L. *J. Mater. Chem.* **2006**, *16*, 1161. (i) Rausch, A. F.; Thompson, M. E.; Yersin, H. *Inorg. Chem.* **2009**, *48*, 1928.

(42) (a) Tamayo, A. B.; Alleyne, B. D.; Djurovich, P. I.; Lamansky, S.; Tsyba, I.; Ho, N. N.; Bau, R.; Thompson, M. E. *J. Am. Chem. Soc.* **2003**, *125*, 7377. (b) Nazeeruddin, M. K.; Humphry-Baker, R.; Berner, D.; Rivier, S.; Zuppiroli, L.; Graetzel, M. *J. Am. Chem. Soc.* **2003**, *125*, 8790. (c) Rausch, A. F.; Thompson, M. E.; Yersin, H. *J. Phys. Chem. A* **2009**, *113*, 5927. (d) Constable, E. C.; Ertl, C. D.; Housecroft, C. E.; Zampese, J. A. *Dalton Trans.* **2014**, *43*, 5343. (e) Colombo, M.; Hauser, A.; Güdel, H. In *Electronic and Vibronic Spectra of Transition Metal Complexes I;* Yersin, H., Ed.; Springer: Berlin, Heidelberg, 1994; Vol. *171*, pp 143. (f) Ragni, R.; Orselli, E.; Kottas, G. S.; Omar, O. H.; Babudri, F.; Pedone, A.; Naso, F.; Farinola, G. M.; De Cola, L. *Chem.—Eur. J.* **2009**, *15*, 136.

(43) (a) Caspar, J. V.; Westmoreland, T. D.; Al1en, G. H.; Brad1ey, P. G.; Meyer, T. J.; Woodruff, W. H. *J. Am. Chem. Soc.* **1984**, *106*, 3492. (b) Miskowski, V. M.; Houlding, V. H.; Che, C.-M.; Wang, Y. *Inorg. Chem.* **1993**, *32*, 2518.

(44) (a) Zuleta, J. A.; Bevilacqua, J. M.; Proserpio, D. M.; Harvey, P. D.; Eisenberg, R. *Inorg. Chem.* **1992**, *31*, 2396. (b) Cummings, S. D.; Eisenberg, R. *Inorg. Chem.* **1995**, *34*, 2007. (c) Connick, W. B.; Gray, H. B. *J. Am. Chem. Soc.* **1997**, *119*, 11620.

DOI: 10.1021/ic502875y
Inorg. Chem. 2015, 54, 2264−2277